# Fixed Beamforming

J. Benesty, I. Cohen, and J. Chen,
*Fundamentals of Signal Enhancement and Array Signal Processing*,
Wiley-IEEE Press, 2017.

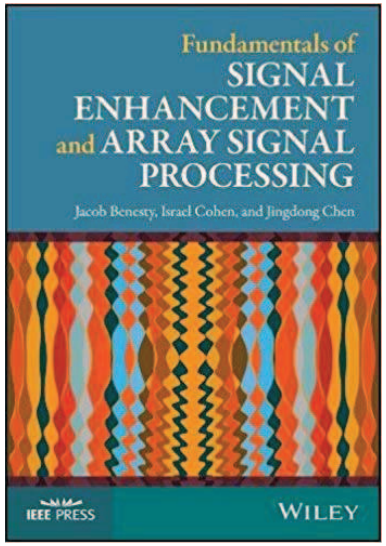

# Outline

# Introduction

A fixed beamformer is a spatial filter that has the ability to form a main beam in the direction of the desired signal and, possibly, place nulls in the directions of interferences.

The coefficients of this filter are fixed and do not depend on the acoustic environment in which the array performs.

Fixed beamforming uses information about the location of the sensors in space and the directions of the desired and interference sources through the steering vectors.

We derive and study a large class of fixed beamformers.

To simplify the presentation of the main results, we consider uniform linear arrays (ULAs).

# Signal Model and Problem Formulation

We consider a plane wave, in the farfield, i.e., far enough from the array, that propagates in an anechoic acoustic environment at the speed of sound, i.e., $c = 340$ m/s, and impinges on a uniform linear sensor array consisting of $M$ omnidirectional microphones.

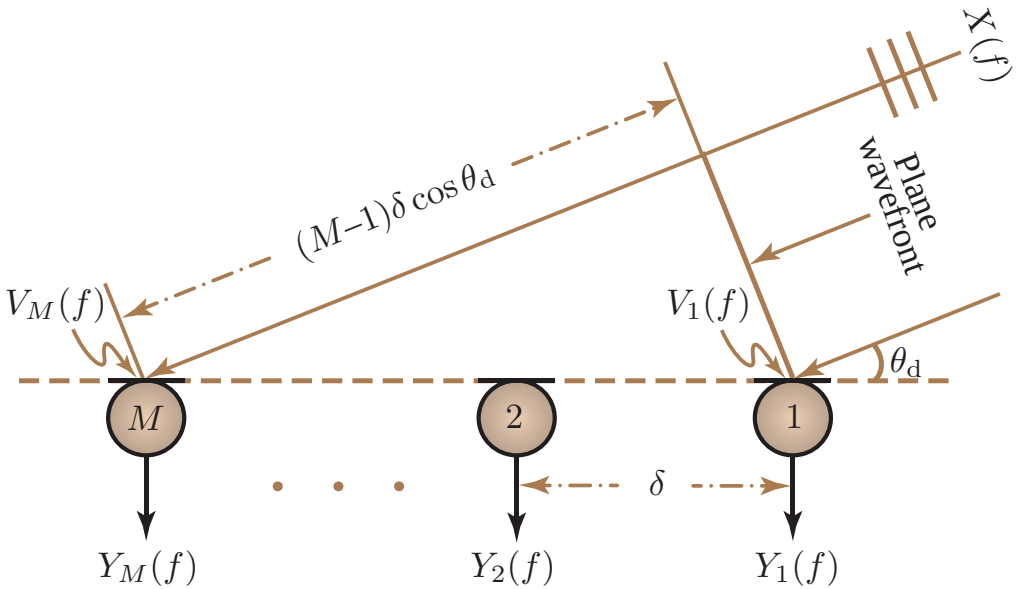


Figure 1: A uniform linear array with $M$ sensors.

The distance between two successive sensors is equal to $\delta$ and the direction of the source signal to the array is parameterized by the azimuth angle $\theta$ (see Fig. 1).

In this context, the steering vector (of length $M$) is given by [1], [2], [3]

$$\mathbf{d}\left(f, \cos\theta\right) = \left[\begin{array}{cccc} 1 & e^{-\jmath 2\pi f \tau_0 \cos\theta} & \cdots & e^{-\jmath(M-1)2\pi f \tau_0 \cos\theta} \end{array}\right]^T, \quad (1)$$

where $\jmath = \sqrt{-1}$ is the imaginary unit, $f > 0$ is the temporal frequency, and $\tau_0 = \delta/c$ is the delay between two successive sensors at the angle $\theta = 0$.

We denote by $\omega = 2\pi f$ the angular frequency and by $\lambda = c/f$ the acoustic wavelength.

Since $\cos\theta$ is an even function so is $\mathbf{d}\left(f, \cos\theta\right)$.

Therefore, the study is limited to angles $\theta \in [0, \pi]$.

Assume that the desired signal propagates from the angle $\theta_{\mathrm{d}}$.

The observation signal vector (of length $M$) is

$$\begin{aligned}\mathbf{y}(f) &= \begin{bmatrix} Y_1(f) & Y_2(f) & \cdots & Y_M(f) \end{bmatrix}^T \\ &= \mathbf{x}(f) + \mathbf{v}(f) \\ &= \mathbf{d}\left(f, \cos\theta_{\mathrm{d}}\right) X(f) + \mathbf{v}(f), \end{aligned} \tag{2}$$

where $Y_m(f)$ is the $m$th microphone signal, $\mathbf{x}(f) = \mathbf{d}\left(f, \cos\theta_{\mathrm{d}}\right) X(f)$, $X(f)$ is the desired signal, $\mathbf{d}\left(f, \cos\theta_{\mathrm{d}}\right)$ is the steering vector at $\theta = \theta_{\mathrm{d}}$ (direction of the desired source), and $\mathbf{v}(f)$ is the additive noise signal vector defined similarly to $\mathbf{y}(f)$.

Then, the correlation matrix of $\mathbf{y}(f)$ is

$$\begin{aligned}\mathbf{\Phi}_{\mathbf{y}}(f) &= E\left[\mathbf{y}(f)\mathbf{y}^H(f)\right] \\ &= \phi_X(f)\mathbf{d}\left(f,\cos\theta_{\mathrm{d}}\right)\mathbf{d}^H\left(f,\cos\theta_{\mathrm{d}}\right)+\mathbf{\Phi}_{\mathbf{v}}(f),\end{aligned} \tag{3}$$

where $\phi_X(f)$ is the variance of $X(f)$ and $\mathbf{\Phi}_{\mathbf{v}}(f)$ is the correlation matrix of $\mathbf{v}(f)$.

Our objective is to design beamformers, independent of the statistics of the signals, which are able to form a main beam in the direction of the desired signal, i.e., $\theta_{\mathrm{d}}$, in order to extract it undistorted while attenuating signals coming from other directions.

# Linear Array Model

Usually, the array processing or beamforming is performed by applying a temporal filter to each microphone signal and summing the filtered signals.

In the frequency domain, this is equivalent to adding a complex weight to the output of each sensor and summing across the aperture [4]:

$$\begin{aligned} Z(f) &= \sum_{m=1}^{M} H_m^*(f) Y_m(f) \\ &= \mathbf{h}^H(f)\mathbf{y}(f) \\ &= X_{\mathrm{fd}}(f) + V_{\mathrm{rn}}(f), \end{aligned} \tag{4}$$

where $Z(f)$ is the beamformer output signal,

$$\mathbf{h}(f) = \begin{bmatrix} H_1(f) & H_2(f) & \cdots & H_M(f) \end{bmatrix}^T \tag{5}$$

is the beamforming weight vector, which is suitable for performing spatial filtering at frequency $f$,

$$X_{\mathrm{fd}}(f) = X(f)\mathbf{h}^H(f)\mathbf{d}\left(f, \cos\theta_{\mathrm{d}}\right) \tag{6}$$

is the filtered desired signal, and

$$V_{\mathrm{rn}}(f) = \mathbf{h}^H(f)\mathbf{v}(f) \tag{7}$$

is the residual noise.

The variance of $Z(f)$ is the sum of two variances:

$$\begin{aligned}\phi_Z(f) &= \mathbf{h}^H(f)\mathbf{\Phi_y}(f)\mathbf{h}(f) \\ &= \phi_{X_{\mathrm{fd}}}(f) + \phi_{V_{\mathrm{rn}}}(f),\end{aligned} \tag{8}$$

where

$$\phi_{X_{\mathrm{fd}}}(f) = \phi_X(f)\left|\mathbf{h}^H(f)\mathbf{d}\left(f,\cos\theta_{\mathrm{d}}\right)\right|^2, \tag{9}$$

$$\phi_{V_{\mathrm{rn}}}(f) = \mathbf{h}^H(f)\mathbf{\Phi_v}(f)\mathbf{h}(f). \tag{10}$$

In the context of fixed beamforming, the distortionless constraint is desired, i.e.,

$$\mathbf{h}^H(f)\mathbf{d}\left(f,\cos\theta_{\mathrm{d}}\right) = 1, \tag{11}$$

meaning that any signal arriving along $\mathbf{d}\left(f,\cos\theta_{\mathrm{d}}\right)$ will pass through the beamformer undistorted.

# Performance Measures
## Beampattern

The beampattern or directivity pattern describes the sensitivity of the beamformer to a plane wave (source signal) impinging on the array from the direction $\theta$.

Mathematically, it is defined as

$$\begin{aligned}\mathcal{B}\left[\mathbf{h}(f), \cos\theta\right] &= \mathbf{d}^H\left(f, \cos\theta\right)\mathbf{h}(f) \\ &= \sum_{m=1}^{M} H_m(f) e^{\jmath(m-1)2\pi f \tau_0 \cos\theta}.\end{aligned} \tag{12}$$

Usually, $\left|\mathcal{B}\left[\mathbf{h}(f), \cos\theta\right]\right|^2$, which is the power pattern [5], is illustrated with a polar plot.

# Signal-to-Noise Ratio

The (narrowband) input SNR is

$$\mathrm{iSNR}(f) = \frac{\phi_X(f)}{\phi_{V_1}(f)}, \tag{13}$$

where $\phi_{V_1}(f) = E\left[|V_1(f)|^2\right]$ is the variance of $V_1(f)$, which is the first element of $\mathbf{v}(f)$.

The (narrowband) output SNR is defined as

$$\begin{aligned}\mathrm{oSNR}\left[\mathbf{h}(f)\right] &= \phi_X(f)\frac{\left|\mathbf{h}^H(f)\mathbf{d}\left(f,\cos\theta_{\mathrm{d}}\right)\right|^2}{\mathbf{h}^H(f)\mathbf{\Phi}_{\mathbf{v}}(f)\mathbf{h}(f)} \\ &= \frac{\phi_X(f)}{\phi_{V_1}(f)} \times \frac{\left|\mathbf{h}^H(f)\mathbf{d}\left(f,\cos\theta_{\mathrm{d}}\right)\right|^2}{\mathbf{h}^H(f)\mathbf{\Gamma}_{\mathbf{v}}(f)\mathbf{h}(f)},\end{aligned} \tag{14}$$

where

$$\mathbf{\Gamma_v}(f) = \frac{\mathbf{\Phi_v}(f)}{\phi_{V_1}(f)} \tag{15}$$

is the pseudo-coherence matrix of $\mathbf{v}(f)$.

From the previous definitions of the SNRs, we deduce the array gain:

$$\begin{aligned} \mathcal{G}\left[\mathbf{h}(f)\right] &= \frac{\mathrm{oSNR}\left[\mathbf{h}(f)\right]}{\mathrm{iSNR}(f)} \\ &= \frac{\left|\mathbf{h}^H(f)\mathbf{d}\left(f, \cos\theta_\mathrm{d}\right)\right|^2}{\mathbf{h}^H(f)\mathbf{\Gamma_v}(f)\mathbf{h}(f)}. \end{aligned} \tag{16}$$

# White Noise Gain

The most convenient way to evaluate the sensitivity of the array to some of its imperfections, such as sensor noise, is via the so-called (narrowband) white noise gain (WNG), which is defined by taking $\mathbf{\Gamma}_{\mathbf{v}}(f) = \mathbf{I}_M$ in (16), where $\mathbf{I}_M$ is the $M \times M$ identity matrix, i.e.,

$$\mathcal{W}\left[\mathbf{h}(f)\right] = \frac{\left|\mathbf{h}^H(f)\mathbf{d}\left(f, \cos\theta_{\mathrm{d}}\right)\right|^2}{\mathbf{h}^H(f)\mathbf{h}(f)}. \tag{17}$$

Using the Cauchy-Schwarz inequality, i.e.,

$$\left|\mathbf{h}^H(f)\mathbf{d}\left(f, \cos\theta_{\mathrm{d}}\right)\right|^2 \leq \mathbf{h}^H(f)\mathbf{h}(f) \times \mathbf{d}^H\left(f, \cos\theta_{\mathrm{d}}\right)\mathbf{d}\left(f, \cos\theta_{\mathrm{d}}\right), \tag{18}$$

we easily deduce from (17) that

$$\mathcal{W}\left[\mathbf{h}(f)\right] \leq M, \ \forall \mathbf{h}(f). \tag{19}$$

As a result, the maximum WNG is

$$\mathcal{W}_{\max} = M, \tag{20}$$

which is frequency independent. Let

$$\cos\left[\mathbf{d}\left(f,\cos\theta_{\mathrm{d}}\right),\mathbf{h}(f)\right] = \frac{\mathbf{d}^{H}\left(f,\cos\theta_{\mathrm{d}}\right)\mathbf{h}(f)+\mathbf{h}^{H}(f)\mathbf{d}\left(f,\cos\theta_{\mathrm{d}}\right)}{2\left\|\mathbf{d}\left(f,\cos\theta_{\mathrm{d}}\right)\right\|_{2}\left\|\mathbf{h}(f)\right\|_{2}} \tag{21}$$

be the cosine of the angle between the two vectors $\mathbf{d}\left(f,\cos\theta_{\mathrm{d}}\right)$ and $\mathbf{h}(f)$, with $\|\cdot\|_2$ denoting the $\ell_2$ norm.

We can rewrite the WNG as

$$\mathcal{W}\left[\mathbf{h}(f)\right] = \mathcal{W}_{\max}\cos^{2}\left[\mathbf{d}\left(f,\cos\theta_{\mathrm{d}}\right),\mathbf{h}(f)\right]. \tag{22}$$

# Directivity Factor

Another important measure, which quantifies how the microphone array performs in the presence of reverberation is the (narrowband) directivity factor (DF).

Considering the spherically isotropic (diffuse) noise field, the DF is defined as [5]

$$\begin{aligned}\mathcal{D}\left[\mathbf{h}(f)\right] &= \frac{\left|\mathcal{B}\left[\mathbf{h}(f),\cos\theta_{\mathrm{d}}\right]\right|^2}{\frac{1}{2}\int_0^{\pi}\left|\mathcal{B}\left[\mathbf{h}(f),\cos\theta\right]\right|^2\sin\theta d\theta} \\ &= \frac{\left|\mathbf{h}^H(f)\mathbf{d}\left(f,\cos\theta_{\mathrm{d}}\right)\right|^2}{\mathbf{h}^H(f)\mathbf{\Gamma}_{0,\pi}(f)\mathbf{h}(f)},\end{aligned} \tag{23}$$

where

$$\mathbf{\Gamma}_{0,\pi}(f) = \frac{1}{2}\int_0^{\pi} \mathbf{d}\left(f, \cos\theta\right) \mathbf{d}^H\left(f, \cos\theta\right) \sin\theta d\theta. \tag{24}$$

It can be verified that the elements of the $M \times M$ matrix $\mathbf{\Gamma}_{0,\pi}(f)$ are

$$\begin{aligned}\left[\mathbf{\Gamma}_{0,\pi}(f)\right]_{ij} &= \frac{\sin\left[2\pi f(j-i)\tau_0\right]}{2\pi f(j-i)\tau_0} \\ &= \operatorname{sinc}\left[2\pi f(j-i)\tau_0\right],\end{aligned} \tag{25}$$

with $\left[\mathbf{\Gamma}_{0,\pi}(f)\right]_{mm} = 1,\ m = 1, 2, \ldots, M$.

Again, by invoking the Cauchy-Schwarz inequality, i.e.,

$$\begin{aligned}\left|\mathbf{h}^H(f)\mathbf{d}\left(f, \cos\theta_{\mathrm{d}}\right)\right|^2 \leq \mathbf{h}^H(f)\mathbf{\Gamma}_{0,\pi}(f)\mathbf{h}(f)\times \\ \mathbf{d}^H\left(f, \cos\theta_{\mathrm{d}}\right)\mathbf{\Gamma}_{0,\pi}^{-1}(f)\mathbf{d}\left(f, \cos\theta_{\mathrm{d}}\right),\end{aligned} \tag{26}$$

we find from (23) that

$$\mathcal{D}\left[\mathbf{h}(f)\right] \leq \mathbf{d}^H\left(f,\cos\theta_{\mathrm{d}}\right)\mathbf{\Gamma}_{0,\pi}^{-1}(f)\mathbf{d}\left(f,\cos\theta_{\mathrm{d}}\right),\ \forall\mathbf{h}(f). \tag{27}$$

As a result, the maximum DF is

$$\begin{aligned}\mathcal{D}_{\max}\left(f,\cos\theta_{\mathrm{d}}\right) &= \mathbf{d}^H\left(f,\cos\theta_{\mathrm{d}}\right)\mathbf{\Gamma}_{0,\pi}^{-1}(f)\mathbf{d}\left(f,\cos\theta_{\mathrm{d}}\right) \\ &= \mathrm{tr}\left[\mathbf{\Gamma}_{0,\pi}^{-1}(f)\mathbf{d}\left(f,\cos\theta_{\mathrm{d}}\right)\mathbf{d}^H\left(f,\cos\theta_{\mathrm{d}}\right)\right] \\ &\leq M\mathrm{tr}\left[\mathbf{\Gamma}_{0,\pi}^{-1}(f)\right],\end{aligned} \tag{28}$$

which is frequency and (desired signal) angle dependent.

Let

$$\cos\left[\mathbf{\Gamma}_{0,\pi}^{-1/2}(f)\mathbf{d}\left(f,\cos\theta_{\mathrm{d}}\right),\mathbf{\Gamma}_{0,\pi}^{1/2}(f)\mathbf{h}(f)\right]=\frac{\mathbf{d}^{H}\left(f,\cos\theta_{\mathrm{d}}\right)\mathbf{h}(f)+\mathbf{h}^{H}(f)\mathbf{d}\left(f,\cos\theta_{\mathrm{d}}\right)}{2\left\|\mathbf{\Gamma}_{0,\pi}^{-1/2}(f)\mathbf{d}\left(f,\cos\theta_{\mathrm{d}}\right)\right\|_{2}\left\|\mathbf{\Gamma}_{0,\pi}^{1/2}(f)\mathbf{h}(f)\right\|_{2}} \tag{29}$$

be the cosine of the angle between the two vectors $\mathbf{\Gamma}_{0,\pi}^{-1/2}(f)\mathbf{d}\left(f,\cos\theta_{\mathrm{d}}\right)$ and $\mathbf{\Gamma}_{0,\pi}^{1/2}(f)\mathbf{h}(f)$.

Then, we can express the DF as

$$\mathcal{D}\left[\mathbf{h}(f)\right]=\mathcal{D}_{\max}\left(f,\cos\theta_{\mathrm{d}}\right)\cos^{2}\left[\mathbf{\Gamma}_{0,\pi}^{-1/2}(f)\mathbf{d}\left(f,\cos\theta_{\mathrm{d}}\right),\mathbf{\Gamma}_{0,\pi}^{1/2}(f)\mathbf{h}(f)\right]. \tag{30}$$

Recall that $\mathbf{h}(f)$ is distortionless, we obtain another formulation of the beampattern:

$$\begin{aligned} \left|\mathcal{B}\left[\mathbf{h}(f), \cos\theta\right]\right|^2 &= \frac{\mathcal{W}_{\max}}{\mathcal{W}\left[\mathbf{h}(f)\right]} \cos^2\left[\mathbf{d}\left(f, \cos\theta\right), \mathbf{h}(f)\right] \\ &= \frac{\mathcal{D}_{\max}\left(f, \cos\theta\right)}{\mathcal{D}\left[\mathbf{h}(f)\right]} \times \\ &\quad \cos^2\left[\mathbf{\Gamma}_{0,\pi}^{-1/2}(f)\mathbf{d}\left(f, \cos\theta\right), \mathbf{\Gamma}_{0,\pi}^{1/2}(f)\mathbf{h}(f)\right]. \end{aligned} \tag{31}$$

This shows how the three fundamental measures, which are the power pattern, the WNG, and the DF, are connected.

# Spatial Aliasing

We discuss here the spatial aliasing problem encountered in array processing; it is similar to the temporal aliasing, which occurs when a continuous-time signal is sampled at a rate lower than twice of its highest frequency.

Let $\theta_1$ and $\theta_2$ be two different angles, i.e., $\theta_1 \neq \theta_2$.

Spatial aliasing occurs when $\mathbf{d}\left(f, \cos\theta_1\right) = \mathbf{d}\left(f, \cos\theta_2\right)$, implying an ambiguity in source locations.

Let

$$\begin{aligned} \cos\theta_1 &= \frac{c}{f\delta} + \cos\theta_2 \\ &= \frac{\lambda}{\delta} + \cos\theta_2, \end{aligned} \tag{32}$$

or, equivalently,

$$\frac{\delta}{\lambda} = \frac{1}{\cos\theta_1 - \cos\theta_2}. \tag{33}$$

It is straightforward to see that

$$e^{-\jmath(m-1)2\pi f\tau_0\cos\theta_1} = e^{-\jmath(m-1)2\pi f\tau_0\cos\theta_2},\ m = 1, 2, \ldots, M. \tag{34}$$

As a consequence,

$$\mathbf{d}\left(f, \cos\theta_1\right) = \mathbf{d}\left(f, \cos\theta_2\right), \tag{35}$$

meaning that spatial aliasing takes place.

Since $|\cos\theta| \leq 1$, we always have

$$|\cos\theta_1 - \cos\theta_2| \leq 2, \tag{36}$$

or, equivalently,

$$\frac{1}{|\cos\theta_1 - \cos\theta_2|} \geq \frac{1}{2}. \tag{37}$$

We conclude from (33) that to prevent aliasing, one needs to ensure that

$$\frac{\delta}{\lambda} < \frac{1}{2}, \tag{38}$$

which is the classical narrowband aliasing criterion.

# Fixed Beamformers

## Delay-and-Sum

In this section, we derive several useful fixed beamformers from the WNG and the DF, which can also be viewed as meaningful criteria as the MSE criterion and not only as performance measures.

The most well-known and popular fixed beamformer is the so-called delay-and-sum (DS), which is derived by maximizing the WNG, i.e.,

$$\min_{\mathbf{h}(f)} \mathbf{h}^H(f)\mathbf{h}(f) \quad \text{subject to} \quad \mathbf{h}^H(f)\mathbf{d}\left(f,\cos\theta_{\mathrm{d}}\right)=1. \tag{39}$$

We easily get the optimal filter:

$$\begin{aligned}\mathbf{h}_{\mathrm{DS}}\left(f,\cos\theta_{\mathrm{d}}\right) &= \frac{\mathbf{d}\left(f,\cos\theta_{\mathrm{d}}\right)}{\mathbf{d}^H\left(f,\cos\theta_{\mathrm{d}}\right)\mathbf{d}\left(f,\cos\theta_{\mathrm{d}}\right)} \\ &= \frac{\mathbf{d}\left(f,\cos\theta_{\mathrm{d}}\right)}{M}.\end{aligned} \tag{40}$$

Therefore, with this beamformer, the WNG and the DF are, respectively,

$$\mathcal{W}\left[\mathbf{h}_{\mathrm{DS}}\left(f,\cos\theta_{\mathrm{d}}\right)\right]=M=\mathcal{W}_{\max} \tag{41}$$

and

$$\mathcal{D}\left[\mathbf{h}_{\mathrm{DS}}\left(f,\cos\theta_{\mathrm{d}}\right)\right]=\frac{M^2}{\mathbf{d}^H\left(f,\cos\theta_{\mathrm{d}}\right)\mathbf{\Gamma}_{0,\pi}(f)\mathbf{d}\left(f,\cos\theta_{\mathrm{d}}\right)}. \tag{42}$$

Since,

$$\mathbf{d}^H\left(f,\cos\theta_{\mathrm{d}}\right)\mathbf{\Gamma}_{0,\pi}(f)\mathbf{d}\left(f,\cos\theta_{\mathrm{d}}\right)\leq M\mathrm{tr}\left[\mathbf{\Gamma}_{0,\pi}(f)\right]=M^2, \tag{43}$$

we have $\mathcal{D}\left[\mathbf{h}_{\mathrm{DS}}\left(f,\cos\theta_{\mathrm{d}}\right)\right]\geq 1$.

While the DS beamformer maximizes the WNG, it never amplifies the diffuse noise since $\mathcal{D}\left[\mathbf{h}_{\mathrm{DS}}\left(f,\cos\theta_{\mathrm{d}}\right)\right]\geq 1$.

We find that the beampattern is

$$\begin{aligned}\left|\mathcal{B}\left[\mathbf{h}_{\mathrm{DS}}\left(f,\cos\theta_{\mathrm{d}}\right),\cos\theta\right]\right|^2 &= \frac{1}{M^2}\left|\mathbf{d}^H\left(f,\cos\theta\right)\mathbf{d}\left(f,\cos\theta_{\mathrm{d}}\right)\right|^2 \qquad (44)\\ &= \frac{1}{M^2}\left|\sum_{m=1}^{M} e^{\jmath(m-1)2\pi f\tau_0(\cos\theta-\cos\theta_{\mathrm{d}})}\right|^2\\ &= \frac{1}{M^2}\left|\frac{1-e^{\jmath M2\pi f\tau_0(\cos\theta-\cos\theta_{\mathrm{d}})}}{1-e^{\jmath 2\pi f\tau_0(\cos\theta-\cos\theta_{\mathrm{d}})}}\right|^2,\end{aligned}$$

with $\left|\mathcal{B}\left[\mathbf{h}_{\mathrm{DS}}\left(f,\cos\theta_{\mathrm{d}}\right),\cos\theta\right]\right|^2 \leq 1$.

The beampattern of the DS beamformer is very frequency dependent.

Let

$$\cos\left[\mathbf{d}\left(f,\cos\theta\right),\mathbf{d}\left(f,\cos\theta_{\mathrm{d}}\right)\right]=\frac{\mathbf{d}^{H}\left(f,\cos\theta\right)\mathbf{d}\left(f,\cos\theta_{\mathrm{d}}\right)+\mathbf{d}^{H}\left(f,\cos\theta_{\mathrm{d}}\right)\mathbf{d}\left(f,\cos\theta\right)}{2\left\|\mathbf{d}\left(f,\cos\theta\right)\right\|_{2}\left\|\mathbf{d}\left(f,\cos\theta_{\mathrm{d}}\right)\right\|_{2}} \tag{45}$$

be the cosine of the angle between the two vectors $\mathbf{d}\left(f,\cos\theta\right)$ and $\mathbf{d}\left(f,\cos\theta_{\mathrm{d}}\right)$.

We can rewrite the beampattern in (44) as

$$\left|\mathcal{B}\left[\mathbf{h}_{\mathrm{DS}}\left(f,\cos\theta_{\mathrm{d}}\right),\cos\theta\right]\right|^{2}=\cos^{2}\left[\mathbf{d}\left(f,\cos\theta\right),\mathbf{d}\left(f,\cos\theta_{\mathrm{d}}\right)\right]. \tag{46}$$

Another interesting way to express (42) is [6]

$$\mathcal{D}\left[\mathbf{h}_{\mathrm{DS}}\left(f,\cos\theta_{\mathrm{d}}\right)\right]=\mathcal{D}_{\max}\left(f,\cos\theta_{\mathrm{d}}\right)\times \cos^{2}\left[\mathbf{\Gamma}_{0,\pi}^{1/2}(f)\mathbf{d}\left(f,\cos\theta_{\mathrm{d}}\right),\mathbf{\Gamma}_{0,\pi}^{-1/2}(f)\mathbf{d}\left(f,\cos\theta_{\mathrm{d}}\right)\right], \tag{47}$$

where

$$\cos\left[\mathbf{\Gamma}_{0,\pi}^{1/2}(f)\mathbf{d}\left(f,\cos\theta_{\mathrm{d}}\right),\mathbf{\Gamma}_{0,\pi}^{-1/2}(f)\mathbf{d}\left(f,\cos\theta_{\mathrm{d}}\right)\right]=\frac{\mathbf{d}^{H}\left(f,\cos\theta_{\mathrm{d}}\right)\mathbf{d}\left(f,\cos\theta_{\mathrm{d}}\right)}{\sqrt{\mathbf{d}^{H}\left(f,\cos\theta_{\mathrm{d}}\right)\mathbf{\Gamma}_{0,\pi}(f)\mathbf{d}\left(f,\cos\theta_{\mathrm{d}}\right)}\sqrt{\mathbf{d}^{H}\left(f,\cos\theta_{\mathrm{d}}\right)\mathbf{\Gamma}_{0,\pi}^{-1}(f)\mathbf{d}\left(f,\cos\theta_{\mathrm{d}}\right)}} \tag{48}$$

is the cosine of the angle between the two vectors $\mathbf{\Gamma}_{0,\pi}^{1/2}(f)\mathbf{d}\left(f,\cos\theta_{\mathrm{d}}\right)$ and $\mathbf{\Gamma}_{0,\pi}^{-1/2}(f)\mathbf{d}\left(f,\cos\theta_{\mathrm{d}}\right)$.

Let $\sigma_1(f)$ and $\sigma_M(f)$ be the maximum and minimum eigenvalues of $\mathbf{\Gamma}_{0,\pi}(f)$, respectively.

Using the Kantorovich inequality [7]:

$$\cos^2\left[\mathbf{\Gamma}_{0,\pi}^{1/2}(f)\mathbf{d}\left(f,\cos\theta_{\mathrm{d}}\right),\mathbf{\Gamma}_{0,\pi}^{-1/2}(f)\mathbf{d}\left(f,\cos\theta_{\mathrm{d}}\right)\right]\geq \frac{4\sigma_1(f)\sigma_M(f)}{\left[\sigma_1(f)+\sigma_M(f)\right]^2}, \tag{49}$$

we deduce that

$$\frac{4\sigma_1(f)\sigma_M(f)}{\left[\sigma_1(f)+\sigma_M(f)\right]^2}\leq\frac{\mathcal{D}\left[\mathbf{h}_{\mathrm{DS}}\left(f,\cos\theta_{\mathrm{d}}\right)\right]}{\mathcal{D}_{\max}\left(f,\cos\theta_{\mathrm{d}}\right)}\leq 1. \tag{50}$$

# Example 1

Consider a ULA of $M$ sensors. Suppose that a desired signal impinges on the ULA from the direction $\theta_{\mathrm{d}}$.

Figure 2 shows plots of the WNG, $\mathcal{W}\left[\mathbf{h}_{\mathrm{DS}}\left(f,\cos\theta_{\mathrm{d}}\right)\right]$, as a function of frequency, for different numbers of sensors, $M$.

Figure 3 shows plots of the DF, $\mathcal{D}\left[\mathbf{h}_{\mathrm{DS}}\left(f,\cos\theta_{\mathrm{d}}\right)\right]$, as a function of frequency, for different numbers of sensors, $M$, and several values of $\theta_{\mathrm{d}}$ and $\delta$.

As the number of sensors increases, both the WNG and the DF of the DS beamformer increase.

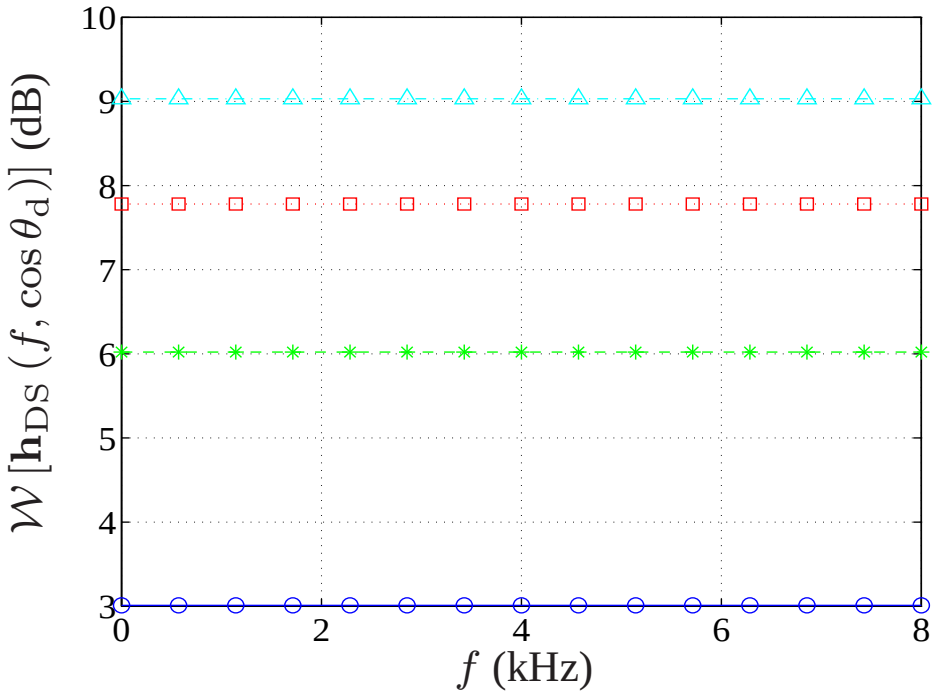


Figure 2: WNG of the DS beamformer for different numbers of sensors, $M$: $M = 2$ (solid line with circles), $M = 4$ (dashed line with asterisks), $M = 6$ (dotted line with squares), and $M = 8$ (dash-dot line with triangles).

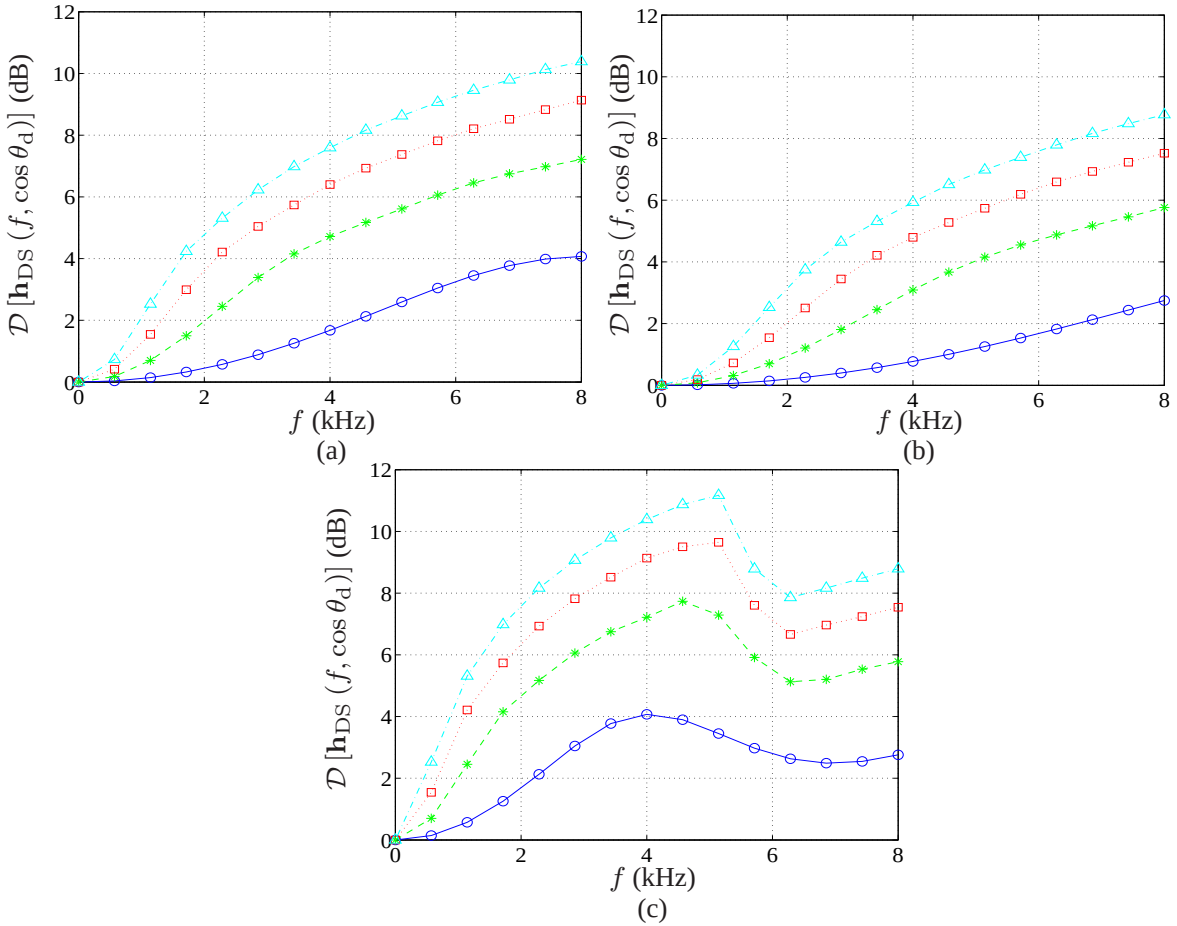


Figure 3: DF of the DS beamformer for different numbers of sensors, $M$, and several values of $\theta_{\mathrm{d}}$ and $\delta$: $M=2$ (solid line with circles), $M=4$ (dashed line with asterisks), $M=6$ (dotted line with squares), and $M=8$ (dash-dot line with triangles). (a) $\theta_{\mathrm{d}}=90^{\circ}$, $\delta=3$ cm, (b) $\theta_{\mathrm{d}}=0^{\circ}$, $\delta=1$ cm, and (c) $\theta_{\mathrm{d}}=0^{\circ}$, $\delta=3$ cm.

Figures 4–6 show beampatterns, $|\mathcal{B}\left[\mathbf{h}_{\mathrm{DS}}\left(f, \cos\theta_{\mathrm{d}}\right), \cos\theta\right]|$, for $M = 8$, several values of $\theta_{\mathrm{d}}$ and $\delta$, and several frequencies.

The main beam is in the direction of the desired signal, i.e., $\theta_{\mathrm{d}}$.

As the frequency increases, the width of the main beam decreases. As $\delta/\lambda$ increases, we may observe spatial aliasing, as demonstrated in Fig. 6(d).

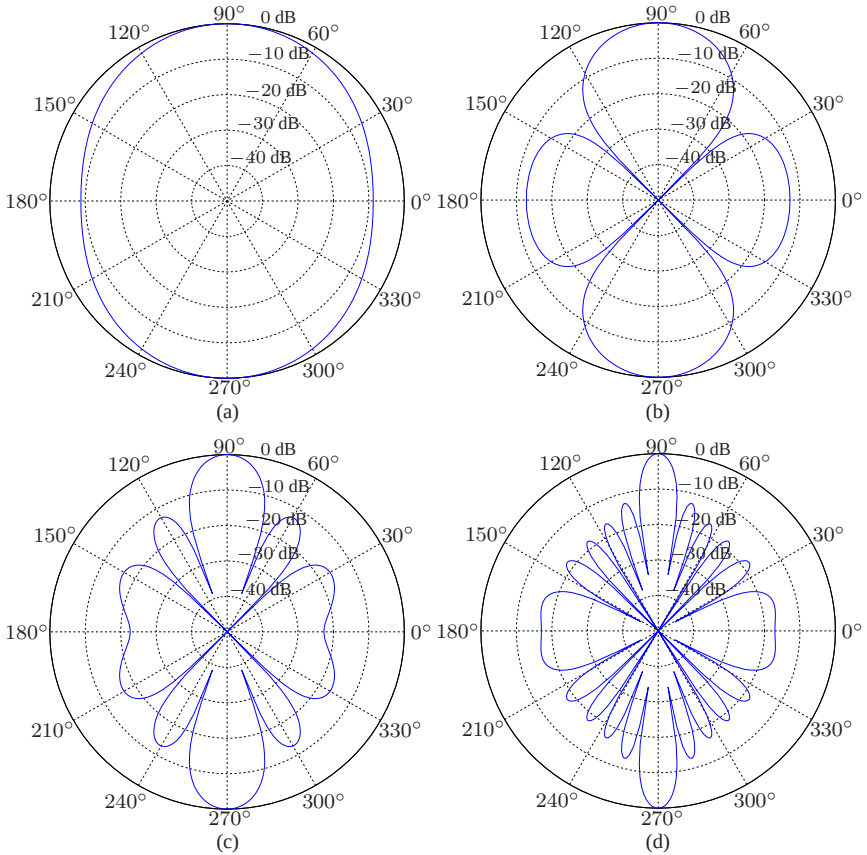


Figure 4: Beampatterns of the DS beamformer for several frequencies with $M = 8$, $\theta_{\mathrm{d}} = 90°$, and $\delta = 3$ cm: (a) $f = 1$ kHz, (b) $f = 2$ kHz, (c) $f = 4$ kHz, and (d) $f = 8$ kHz.

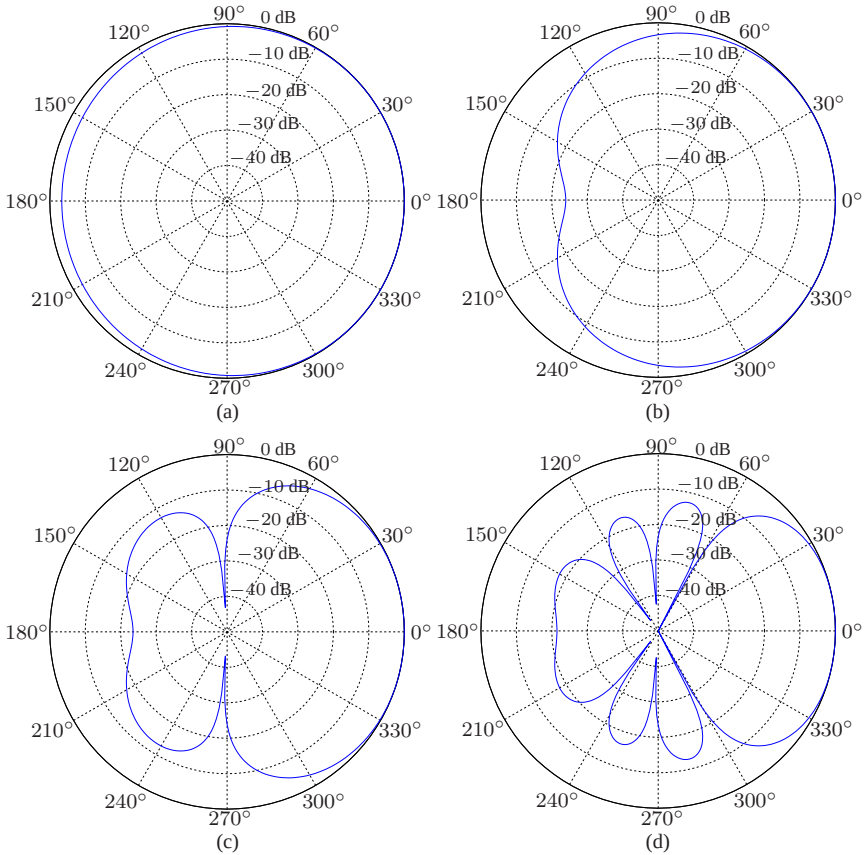


Figure 5: Beampatterns of the DS beamformer for several frequencies with $M = 8$, $\theta_{\mathrm{d}} = 0°$, and $\delta = 1$ cm: (a) $f = 1$ kHz, (b) $f = 2$ kHz, (c) $f = 4$ kHz, and (d) $f = 8$ kHz.

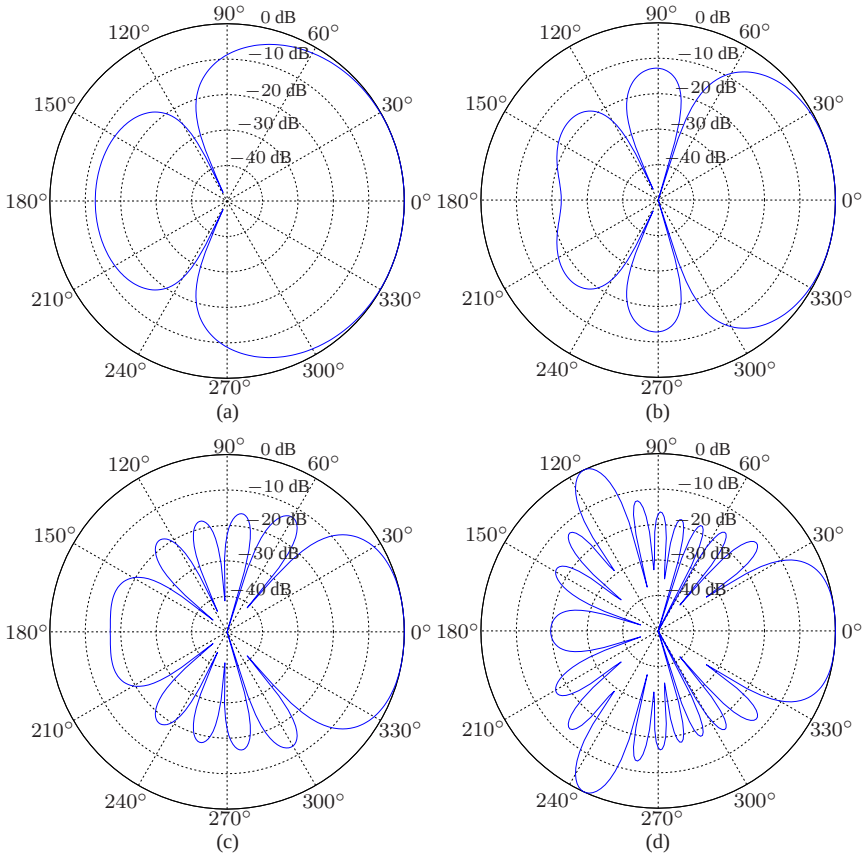


Figure 6: Beampatterns of the DS beamformer for several frequencies with $M = 8$, $\theta_{\mathrm{d}} = 0°$, and $\delta = 3$ cm: (a) $f = 1$ kHz, (b) $f = 2$ kHz, (c) $f = 4$ kHz, and (d) $f = 8$ kHz.

# Maximum DF

The maximum DF beamformer, as the name implies, maximizes the DF, i.e.,

$$\min_{\mathbf{h}(f)} \mathbf{h}^H(f)\mathbf{\Gamma}_{0,\pi}(f)\mathbf{h}(f) \quad \text{subject to} \quad \mathbf{h}^H(f)\mathbf{d}\left(f,\cos\theta_{\mathrm{d}}\right)=1. \tag{51}$$

Then, the maximum DF beamformer is

$$\mathbf{h}_{\mathrm{mDF}}\left(f,\cos\theta_{\mathrm{d}}\right)=\frac{\mathbf{\Gamma}_{0,\pi}^{-1}(f)\mathbf{d}\left(f,\cos\theta_{\mathrm{d}}\right)}{\mathbf{d}^H\left(f,\cos\theta_{\mathrm{d}}\right)\mathbf{\Gamma}_{0,\pi}^{-1}(f)\mathbf{d}\left(f,\cos\theta_{\mathrm{d}}\right)}. \tag{52}$$

We deduce that the WNG and the DF are, respectively,

$$\mathcal{W}\left[\mathbf{h}_{\mathrm{mDF}}\left(f,\cos\theta_{\mathrm{d}}\right)\right]=\frac{\left[\mathbf{d}^{H}\left(f,\cos\theta_{\mathrm{d}}\right)\mathbf{\Gamma}_{0,\pi}^{-1}(f)\mathbf{d}\left(f,\cos\theta_{\mathrm{d}}\right)\right]^{2}}{\mathbf{d}^{H}\left(f,\cos\theta_{\mathrm{d}}\right)\mathbf{\Gamma}_{0,\pi}^{-2}(f)\mathbf{d}\left(f,\cos\theta_{\mathrm{d}}\right)} \tag{53}$$

and

$$\begin{aligned}\mathcal{D}\left[\mathbf{h}_{\mathrm{mDF}}\left(f,\cos\theta_{\mathrm{d}}\right)\right]&=\mathbf{d}^{H}\left(f,\cos\theta_{\mathrm{d}}\right)\mathbf{\Gamma}_{0,\pi}^{-1}(f)\mathbf{d}\left(f,\cos\theta_{\mathrm{d}}\right)\\&=\mathcal{D}_{\max}\left(f,\cos\theta_{\mathrm{d}}\right).\end{aligned} \tag{54}$$

It is not hard to see that the beampattern is

$$\left|\mathcal{B}\left[\mathbf{h}_{\mathrm{mDF}}\left(f,\cos\theta_{\mathrm{d}}\right),\cos\theta\right]\right|^{2}=\frac{\left|\mathbf{d}^{H}\left(f,\cos\theta\right)\mathbf{\Gamma}_{0,\pi}^{-1}(f)\mathbf{d}\left(f,\cos\theta_{\mathrm{d}}\right)\right|^{2}}{\left[\mathbf{d}^{H}\left(f,\cos\theta_{\mathrm{d}}\right)\mathbf{\Gamma}_{0,\pi}^{-1}(f)\mathbf{d}\left(f,\cos\theta_{\mathrm{d}}\right)\right]^{2}}, \tag{55}$$

which can be rewritten as

$$\left|\mathcal{B}\left[\mathbf{h}_{\mathrm{mDF}}\left(f,\cos\theta_{\mathrm{d}}\right),\cos\theta\right]\right|^{2}=\frac{\mathcal{D}_{\max}\left(f,\cos\theta\right)}{\mathcal{D}_{\max}\left(f,\cos\theta_{\mathrm{d}}\right)}\times\cos^{2}\left[\boldsymbol{\Gamma}_{0,\pi}^{-1/2}(f)\mathbf{d}\left(f,\cos\theta\right),\boldsymbol{\Gamma}_{0,\pi}^{-1/2}(f)\mathbf{d}\left(f,\cos\theta_{\mathrm{d}}\right)\right], \tag{56}$$

where

$$\cos\left[\boldsymbol{\Gamma}_{0,\pi}^{-1/2}(f)\mathbf{d}\left(f,\cos\theta\right),\boldsymbol{\Gamma}_{0,\pi}^{-1/2}(f)\mathbf{d}\left(f,\cos\theta_{\mathrm{d}}\right)\right]=\frac{\mathbf{d}^{H}\left(f,\cos\theta\right)\boldsymbol{\Gamma}_{0,\pi}^{-1}(f)\mathbf{d}\left(f,\cos\theta_{\mathrm{d}}\right)+\mathbf{d}^{H}\left(f,\cos\theta_{\mathrm{d}}\right)\boldsymbol{\Gamma}_{0,\pi}^{-1}(f)\mathbf{d}\left(f,\cos\theta\right)}{2\left\|\boldsymbol{\Gamma}_{0,\pi}^{-1/2}(f)\mathbf{d}\left(f,\cos\theta\right)\right\|_{2}\left\|\boldsymbol{\Gamma}_{0,\pi}^{-1/2}(f)\mathbf{d}\left(f,\cos\theta_{\mathrm{d}}\right)\right\|_{2}} \tag{57}$$

is the cosine of the angle between the two vectors $\boldsymbol{\Gamma}_{0,\pi}^{-1/2}(f)\mathbf{d}\left(f,\cos\theta\right)$ and $\boldsymbol{\Gamma}_{0,\pi}^{-1/2}(f)\mathbf{d}\left(f,\cos\theta_{\mathrm{d}}\right)$.

We can observe from (56) that $\left|\mathcal{B}\left[\mathbf{h}_{\mathrm{mDF}}\left(f,\cos\theta_{\mathrm{d}}\right),\cos\theta\right]\right|^2$ may not be necessarily smaller than $1$.

We can express the WNG as [6]

$$\mathcal{W}\left[\mathbf{h}_{\mathrm{mDF}}\left(f,\cos\theta_{\mathrm{d}}\right)\right]=\mathcal{W}_{\max}\cos^2\left[\mathbf{d}\left(f,\cos\theta_{\mathrm{d}}\right),\mathbf{\Gamma}_{0,\pi}^{-1}(f)\mathbf{d}\left(f,\cos\theta_{\mathrm{d}}\right)\right], \tag{58}$$

where

$$\cos\left[\mathbf{d}\left(f,\cos\theta_{\mathrm{d}}\right),\mathbf{\Gamma}_{0,\pi}^{-1}(f)\mathbf{d}\left(f,\cos\theta_{\mathrm{d}}\right)\right]= \frac{\mathbf{d}^H\left(f,\cos\theta_{\mathrm{d}}\right)\mathbf{\Gamma}_{0,\pi}^{-1}(f)\mathbf{d}\left(f,\cos\theta_{\mathrm{d}}\right)}{\sqrt{\mathbf{d}^H\left(f,\cos\theta_{\mathrm{d}}\right)\mathbf{d}\left(f,\cos\theta_{\mathrm{d}}\right)}\sqrt{\mathbf{d}^H\left(f,\cos\theta_{\mathrm{d}}\right)\mathbf{\Gamma}_{0,\pi}^{-2}(f)\mathbf{d}\left(f,\cos\theta_{\mathrm{d}}\right)}} \tag{59}$$

is the cosine of the angle between the two vectors $\mathbf{d}\left(f,\cos\theta_{\mathrm{d}}\right)$ and $\mathbf{\Gamma}_{0,\pi}^{-1}(f)\left(f,\cos\theta_{\mathrm{d}}\right)$.

Again, by invoking the Kantorovich inequality, we find that

$$\frac{4\sigma_1(f)\sigma_M(f)}{\left[\sigma_1(f)+\sigma_M(f)\right]^2} \leq \frac{\mathcal{W}\left[\mathbf{h}_{\mathrm{mDF}}\left(f,\cos\theta_{\mathrm{d}}\right)\right]}{\mathcal{W}_{\max}} \leq 1. \tag{60}$$

We can see from (58) that the WNG may be smaller than $1$, which implies white noise amplification.

It is interesting to observe that

$$\frac{1}{\mathbf{h}_{\mathrm{mDF}}^H\left(f,\cos\theta_{\mathrm{d}}\right)\mathbf{h}_{\mathrm{DS}}\left(f,\cos\theta_{\mathrm{d}}\right)} = \mathcal{W}_{\max} \tag{61}$$

and

$$\frac{1}{\mathbf{h}_{\mathrm{mDF}}^H\left(f,\cos\theta_{\mathrm{d}}\right)\mathbf{\Gamma}_{0,\pi}(f)\mathbf{h}_{\mathrm{DS}}\left(f,\cos\theta_{\mathrm{d}}\right)} = \mathcal{D}_{\max}\left(f,\cos\theta_{\mathrm{d}}\right). \tag{62}$$

We also give the obvious relationship between the DS and maximum DF beamformers:

$$\mathcal{D}_{\max}\left(f,\cos\theta_{\mathrm{d}}\right)\mathbf{\Gamma}_{0,\pi}\left(f\right)\mathbf{h}_{\mathrm{mDF}}\left(f,\cos\theta_{\mathrm{d}}\right)=\mathcal{W}_{\max}\mathbf{h}_{\mathrm{DS}}\left(f,\cos\theta_{\mathrm{d}}\right). \quad (63)$$

# Example 2

Returning to Example 1, we now employ the maximum DF beamformer, $\mathbf{h}_{\mathrm{mDF}}\left(f, \cos\theta_{\mathrm{d}}\right)$, given in (52).

Figure 7 shows plots of the WNG, $\mathcal{W}\left[\mathbf{h}_{\mathrm{mDF}}\left(f, \cos\theta_{\mathrm{d}}\right)\right]$, as a function of frequency, for different numbers of sensors, $M$, and several values of $\theta_{\mathrm{d}}$ and $\delta$.

Figure 8 shows plots of the DF, $\mathcal{D}\left[\mathbf{h}_{\mathrm{mDF}}\left(f, \cos\theta_{\mathrm{d}}\right)\right]$, as a function of frequency, for different numbers of sensors, $M$, and several values of $\theta_{\mathrm{d}}$ and $\delta$.

Compared to the DS beamformer, the maximum DF beamformer obtains higher DF, but lower WNG (cf. Figs. 2 and 3).

Generally, for high frequencies, as the number of sensors increases, both the DF and the WNG of the maximum DF beamformer increase.

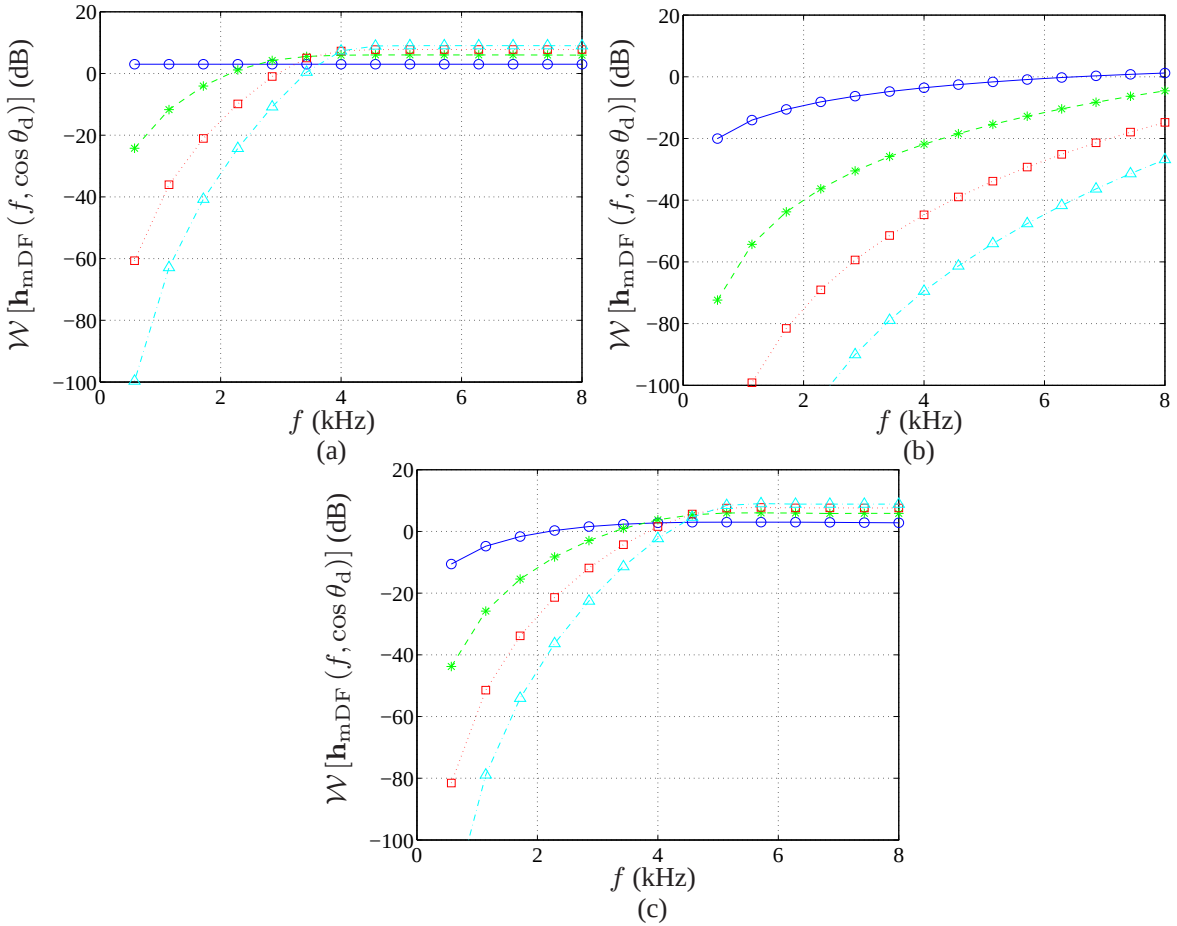


Figure 7: WNG of the maximum DF beamformer for different numbers of sensors, $M$, and several values of $\theta_{\mathrm{d}}$ and $\delta$: $M = 2$ (solid line with circles), $M = 4$ (dashed line with asterisks), $M = 6$ (dotted line with squares), and $M = 8$ (dash-dot line with triangles). (a) $\theta_{\mathrm{d}} = 90°$, $\delta = 3$ cm, (b) $\theta_{\mathrm{d}} = 0°$, $\delta = 1$ cm, and (c) $\theta_{\mathrm{d}} = 0°$, $\delta = 3$ cm.

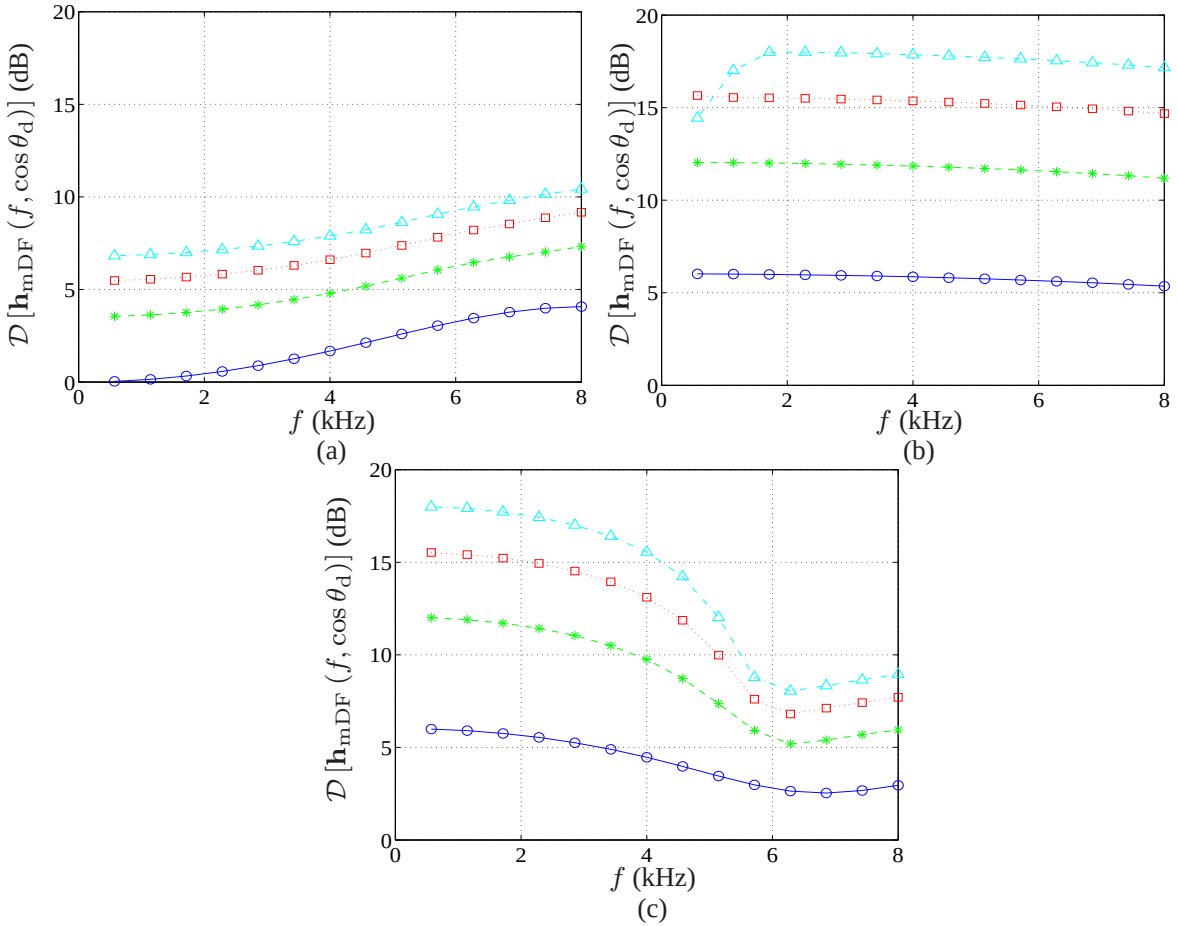


Figure 8: DF of the maximum DF beamformer for different numbers of sensors, $M$, and several values of $\theta_{\mathrm{d}}$ and $\delta$: $M = 2$ (solid line with circles), $M = 4$ (dashed line with asterisks), $M = 6$ (dotted line with squares), and $M = 8$ (dash-dot line with triangles). (a) $\theta_{\mathrm{d}} = 90°$, $\delta = 3$ cm, (b) $\theta_{\mathrm{d}} = 0°$, $\delta = 1$ cm, and (c) $\theta_{\mathrm{d}} = 0°$, $\delta = 3$ cm.

Figures 9–11 show beampatterns, $|\mathcal{B}\left[\mathbf{h}_{\mathrm{mDF}}\left(f, \cos\theta_{\mathrm{d}}\right), \cos\theta\right]|$, for $M = 8$, several values of $\theta_{\mathrm{d}}$ and $\delta$, and several frequencies.

The main beam is in the direction of the desired signal, i.e., $\theta_{\mathrm{d}}$.

As the frequency increases, the width of the main beam decreases.

As $\delta/\lambda$ increases, we may observe spatial aliasing, as demonstrated in Fig. 11(d).

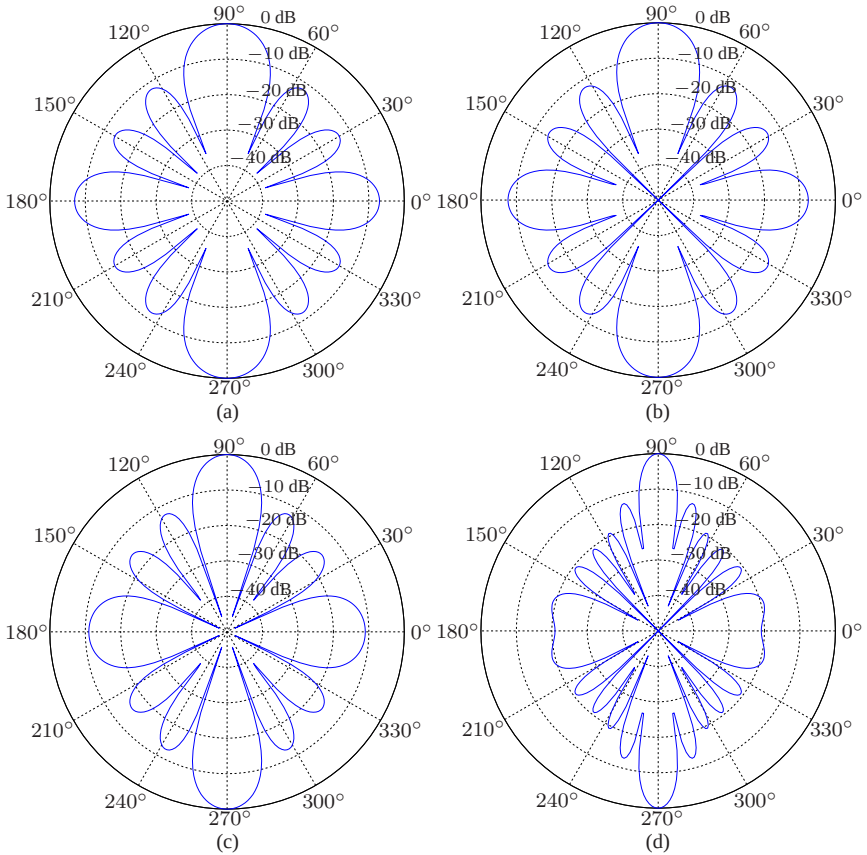


Figure 9: Beampatterns of the maximum DF beamformer for several frequencies with $M = 8$, $\theta_{\mathrm{d}} = 90°$, and $\delta = 3$ cm: (a) $f = 1$ kHz, (b) $f = 2$ kHz, (c) $f = 4$ kHz, and (d) $f = 8$ kHz.

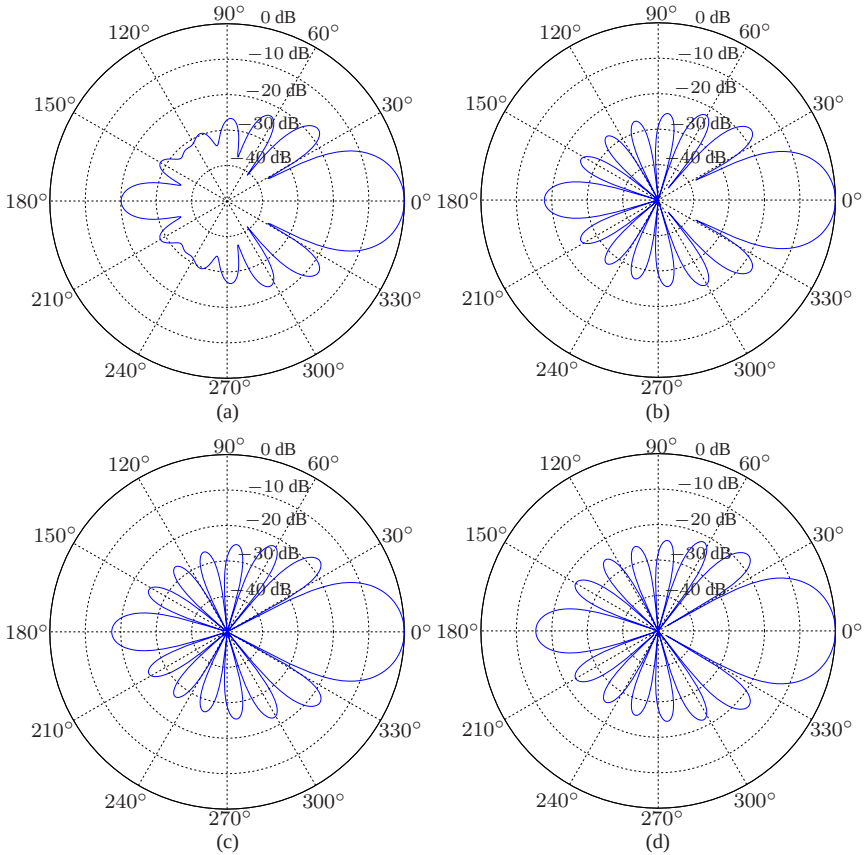


Figure 10: Beampatterns of the maximum DF beamformer for several frequencies with $M = 8$, $\theta_{\mathrm{d}} = 0°$, and $\delta = 1$ cm: (a) $f = 1$ kHz, (b) $f = 2$ kHz, (c) $f = 4$ kHz, and (d) $f = 8$ kHz.

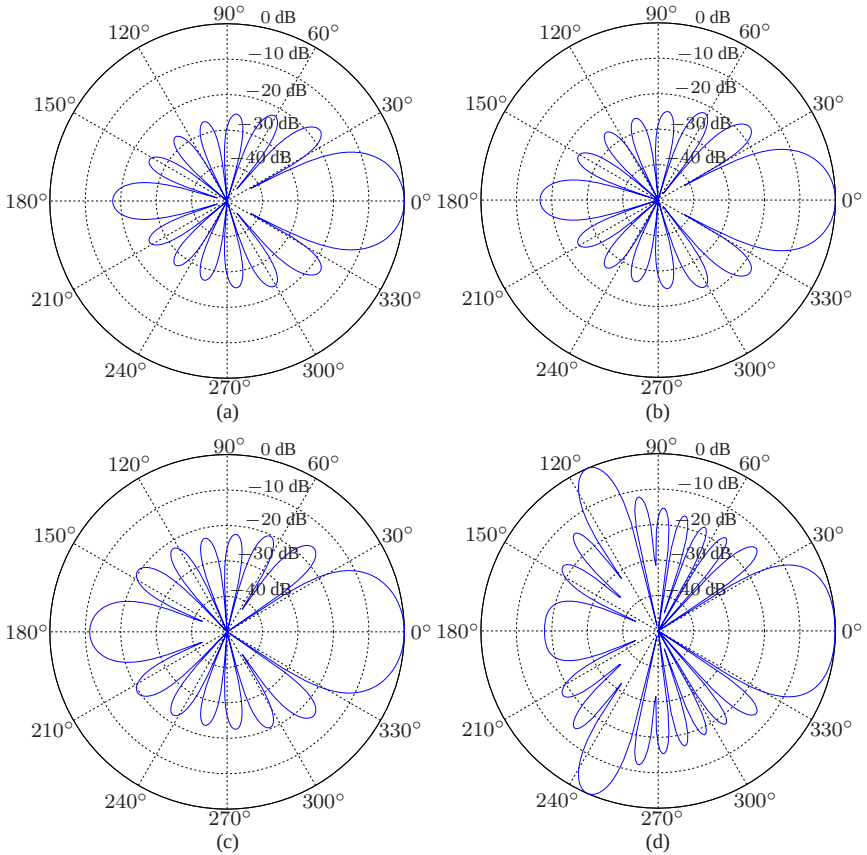


Figure 11: Beampatterns of the maximum DF beamformer for several frequencies with $M = 8$, $\theta_{\mathrm{d}} = 0°$, and $\delta = 3$ cm: (a) $f = 1$ kHz, (b) $f = 2$ kHz, (c) $f = 4$ kHz, and (d) $f = 8$ kHz.

# Superdirective

Let us evaluate the maximum DF, which is also the DF of the maximum DF beamformer, for $M = 2$.

After simple algebraic manipulations, we find that

$$\mathcal{D}_{\max}\left(f, \cos\theta_{\mathrm{d}}\right) = 2\frac{1 - \operatorname{sinc}\left(2\pi f\tau_0\right)\cos\left(2\pi f\tau_0\cos\theta_{\mathrm{d}}\right)}{1 - \operatorname{sinc}^2\left(2\pi f\tau_0\right)}. \tag{64}$$

Using in (64) the approximations:

$$\operatorname{sinc} x \approx 1 - \frac{x^2}{6}, \tag{65}$$

$$\cos x \approx 1 - \frac{x^2}{2}, \tag{66}$$

we obtain

$$\mathcal{D}_{\max}\left(f,\cos\theta_{\mathrm{d}}\right)\approx\frac{6\left[6\cos^{2}\theta_{\mathrm{d}}+2-\left(2\pi f\tau_{0}\right)^{2}\cos^{2}\theta_{\mathrm{d}}\right]}{12-\left(2\pi f\tau_{0}\right)^{2}}. \tag{67}$$

First, for $\delta$ very small, the previous expression can be further approximated by

$$\mathcal{D}_{\max}\left(f,\cos\theta_{\mathrm{d}}\right)\approx 3\cos^{2}\theta_{\mathrm{d}}+1, \tag{68}$$

which is frequency independent.

Second, it is clear from (68) that the maximum DF is maximized for $\theta_{\mathrm{d}}=0$ or $\pi$ (endfire direction).

The minimum of the maximum DF is obtained for $\theta_{\mathrm{d}}=\pi/2$ (broadside direction).

From this simple example, we can conclude, that the best arrays as far the DF is concerned, are endfire arrays with a small interelement spacing.

Broadside arrays do not perform very well in general.

A deeper study in [8] draws the same conclusions.

Other experimental studies show the benefits of endfire arrays [9].

In fact, it can be shown that [10]

$$\lim_{\delta \to 0} \mathcal{D}_{\max}(f, 1) = M^2. \tag{69}$$

This high DF is called supergain in the literature.

The well-known superdirective beamformer is just a particular case of the maximum DF beamformer, where $\theta_{\mathrm{d}} = 0$ and $\delta$ is small.

It is given by [11]

$$\mathbf{h}_{\mathrm{SD}}(f) = \frac{\mathbf{\Gamma}_{0,\pi}^{-1}(f)\mathbf{d}\left(f,1\right)}{\mathbf{d}^{H}\left(f,1\right)\mathbf{\Gamma}_{0,\pi}^{-1}(f)\mathbf{d}\left(f,1\right)}. \tag{70}$$

While the superdirective beamformer maximizes the DF, it may amplify the white noise, i.e., the WNG may be smaller than 1, especially at low frequencies [see Figs. 7(b) and (c)].

# Robust Superdirective

It is well known that the superdirective beamformer is sensitive to the spatially white noise, so it lacks robustness.

In order to deal with this important problem, the authors in [11], [12] proposed to maximize the DF:

$$\mathcal{D}\left[\mathbf{h}(f)\right] = \frac{\left|\mathbf{h}^H(f)\mathbf{d}\left(f,1\right)\right|^2}{\mathbf{h}^H(f)\mathbf{\Gamma}_{0,\pi}(f)\mathbf{h}(f)}, \tag{71}$$

subject to a constraint on the WNG:

$$\mathcal{W}\left[\mathbf{h}(f)\right] = \frac{\left|\mathbf{h}^H(f)\mathbf{d}\left(f,1\right)\right|^2}{\mathbf{h}^H(f)\mathbf{h}(f)}. \tag{72}$$

This is equivalent to minimizing $1/\mathcal{D}\left[\mathbf{h}(f)\right]$ with a constraint on $1/\mathcal{W}\left[\mathbf{h}(f)\right]$, i.e., minimizing

$$\frac{1}{\mathcal{D}\left[\mathbf{h}(f)\right]}+\epsilon\frac{1}{\mathcal{W}\left[\mathbf{h}(f)\right]}=\frac{\mathbf{h}^{H}(f)\left[\mathbf{\Gamma}_{0,\pi}(f)+\epsilon\mathbf{I}_{M}\right]\mathbf{h}(f)}{\left|\mathbf{h}^{H}(f)\mathbf{d}\left(f,1\right)\right|^{2}}, \tag{73}$$

where $\epsilon\geq 0$ is a Lagrange multiplier.

Using the distortionless constraint, we easily find that the optimal solution is

$$\mathbf{h}_{\mathrm{R},\epsilon}(f)=\frac{\left[\mathbf{\Gamma}_{0,\pi}(f)+\epsilon\mathbf{I}_{M}\right]^{-1}\mathbf{d}\left(f,1\right)}{\mathbf{d}^{H}\left(f,1\right)\left[\mathbf{\Gamma}_{0,\pi}(f)+\epsilon\mathbf{I}_{M}\right]^{-1}\mathbf{d}\left(f,1\right)}. \tag{74}$$

It is clear that (74) is a regularized version of (70), where $\epsilon$ is the regularization parameter.

This parameter tries to find a good compromise between a supergain and white noise amplification.

A small $\epsilon$ leads to a large DF and a low WNG, while a large $\epsilon$ gives a low DF and a large WNG.

We have $\mathbf{h}_{\mathrm{R},0}(f) = \mathbf{h}_{\mathrm{SD}}(f)$ and $\mathbf{h}_{\mathrm{R},\infty}(f) = \mathbf{h}_{\mathrm{DS}}(f,1)$.

In practice, since white noise amplification is much worse at low frequencies than at high frequencies, it is better to make $\epsilon$ frequency dependent.

Therefore, (74) is rewritten as

$$\mathbf{h}_{\mathrm{R},\epsilon}(f) = \frac{\left[\mathbf{\Gamma}_{0,\pi}(f) + \epsilon(f)\mathbf{I}_M\right]^{-1}\mathbf{d}\left(f,1\right)}{\mathbf{d}^H\left(f,1\right)\left[\mathbf{\Gamma}_{0,\pi}(f) + \epsilon(f)\mathbf{I}_M\right]^{-1}\mathbf{d}\left(f,1\right)}. \tag{75}$$

An equivalent way to express (75) is

$$\mathbf{h}_{\mathrm{R},\alpha}(f) = \frac{\mathbf{\Gamma}_{\alpha}^{-1}(f)\mathbf{d}\left(f,1\right)}{\mathbf{d}^{H}\left(f,1\right)\mathbf{\Gamma}_{\alpha}^{-1}(f)\mathbf{d}\left(f,1\right)}, \tag{76}$$

where

$$\mathbf{\Gamma}_{\alpha}(f) = \left[1-\alpha(f)\right]\mathbf{\Gamma}_{0,\pi}(f) + \alpha(f)\mathbf{I}_{M}, \tag{77}$$

with $\alpha(f)$ being a real number and $0 \leq \alpha(f) \leq 1$.

It can be checked that the relationship between $\alpha(f)$ and $\epsilon(f)$ is

$$\epsilon(f) = \frac{\alpha(f)}{1-\alpha(f)}. \tag{78}$$

The robust superdirective beamformer given in (76) may be preferable to use in practice than its equivalent form given in (75) since $\alpha(f)$ is chosen only from $0$ to $1$ in the former while $\epsilon(f)$ is chosen from $0$ to $\infty$ in the latter.

We find that the WNG and the DF are, respectively,

$$\mathcal{W}\left[\mathbf{h}_{\mathrm{R},\alpha}(f)\right] = \frac{\left[\mathbf{d}^H(f,1)\,\mathbf{\Gamma}_\alpha^{-1}(f)\mathbf{d}(f,1)\right]^2}{\mathbf{d}^H(f,1)\,\mathbf{\Gamma}_\alpha^{-2}(f)\mathbf{d}(f,1)} \tag{79}$$

and

$$\mathcal{D}\left[\mathbf{h}_{\mathrm{R},\alpha}(f)\right] = \frac{\left[\mathbf{d}^H(f,1)\,\mathbf{\Gamma}_\alpha^{-1}(f)\mathbf{d}(f,1)\right]^2}{\mathbf{d}^H(f,1)\,\mathbf{\Gamma}_\alpha^{-1}(f)\mathbf{\Gamma}_{0,\pi}(f)\mathbf{\Gamma}_\alpha^{-1}(f)\mathbf{d}(f,1)}. \tag{80}$$

Using the geometrical interpretation, the two previous expressions are also

$$\mathcal{W}\left[\mathbf{h}_{\mathrm{R},\alpha}(f)\right] = \mathcal{W}_{\max}\cos^2\left[\mathbf{d}\left(f,1\right),\mathbf{\Gamma}_{\alpha}^{-1}(f)\mathbf{d}\left(f,1\right)\right] \tag{81}$$

and

$$\mathcal{D}\left[\mathbf{h}_{\mathrm{R},\alpha}(f)\right] = \mathcal{D}_{\max}\left(f,1\right)\times \cos^2\left[\mathbf{\Gamma}_{0,\pi}^{1/2}(f)\mathbf{\Gamma}_{\alpha}^{-1}(f)\mathbf{d}\left(f,1\right),\mathbf{\Gamma}_{0,\pi}^{-1/2}(f)\mathbf{d}\left(f,1\right)\right]. \tag{82}$$

The beampattern of the robust superdirective beamformer is

$$\begin{aligned}\left|\mathcal{B}\left[\mathbf{h}_{\mathrm{R},\alpha}(f),\cos\theta\right]\right|^2 &= \frac{\left|\mathbf{d}^H\left(f,\cos\theta\right)\mathbf{\Gamma}_\alpha^{-1}(f)\mathbf{d}\left(f,1\right)\right|^2}{\left[\mathbf{d}^H\left(f,\cos 1\right)\mathbf{\Gamma}_\alpha^{-1}(f)\mathbf{d}\left(f,1\right)\right]^2} \\ &= \frac{\mathcal{D}_{\max,\alpha}\left(f,1\right)}{\mathcal{D}_{\max,\alpha}\left(f,\cos\theta\right)}\times \\ &\quad \cos^2\left[\mathbf{\Gamma}_\alpha^{-1/2}(f)\mathbf{d}\left(f,\cos\theta\right),\mathbf{\Gamma}_\alpha^{-1/2}(f)\mathbf{d}\left(f,1\right)\right],\end{aligned} \tag{83}$$

where

$$\mathcal{D}_{\max,\alpha}\left(f,\cos\theta\right) = \mathbf{d}^H\left(f,\cos\theta\right)\mathbf{\Gamma}_\alpha^{-1}(f)\mathbf{d}\left(f,\cos\theta\right). \tag{84}$$

# Example 3

Returning to Example 1, we now employ the robust superdirective beamformer, $\mathbf{h}_{\mathrm{R},\alpha}(f)$, given in (76).

To demonstrate the performance of the robust superdirective beamformer, we choose $\delta = 1$ cm.

Figure 12 shows plots of the WNG, $\mathcal{W}\left[\mathbf{h}_{\mathrm{R},\alpha}(f)\right]$, as a function of frequency, for different numbers of sensors, $M$, and several values of $\alpha$.

Figure 13 shows plots of the WNG, $\mathcal{W}\left[\mathbf{h}_{\mathrm{R},\alpha}(f)\right]$, as a function of $\alpha$, for different numbers of sensors, $M$, and several frequencies.

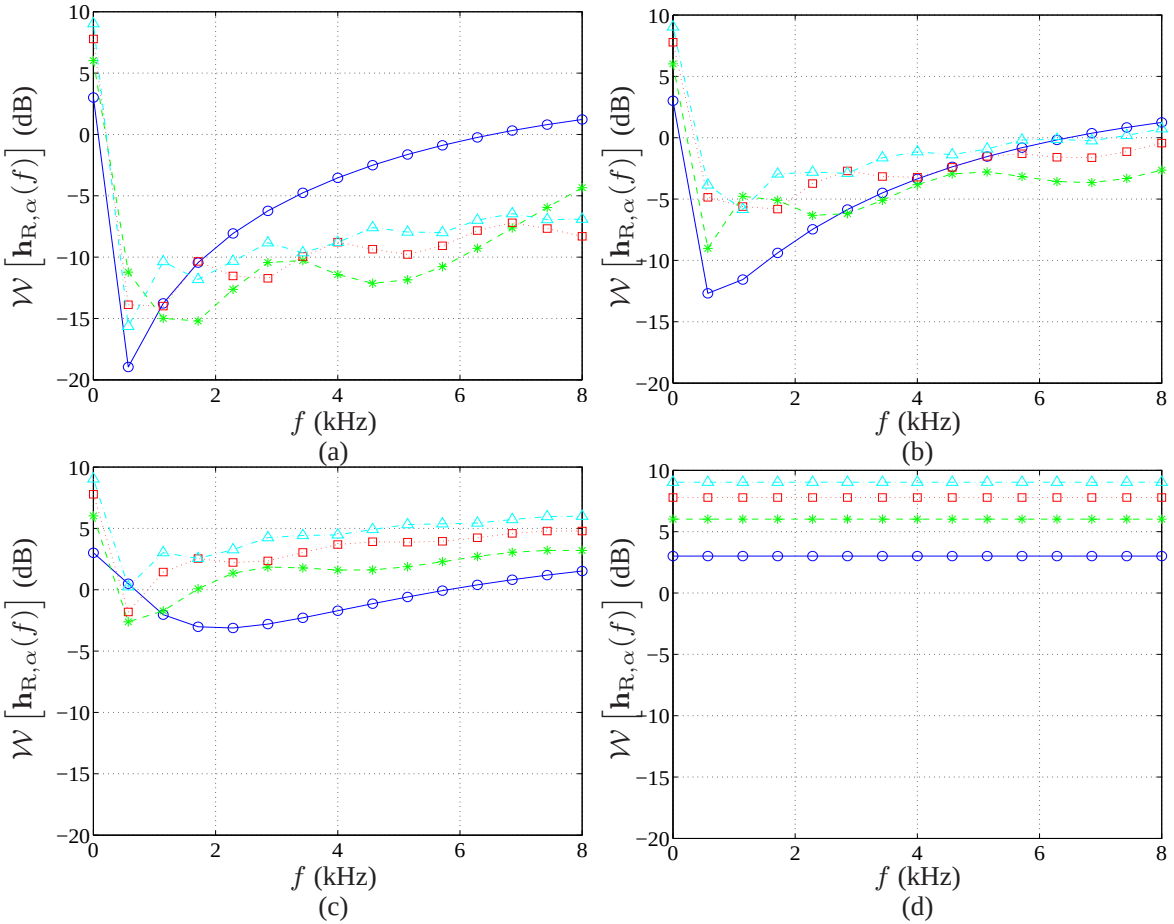


Figure 12: WNG of the robust superdirective beamformer for different numbers of sensors, $M$, and several values of $\alpha$: $M = 2$ (solid line with circles), $M = 4$ (dashed line with asterisks), $M = 6$ (dotted line with squares), and $M = 8$ (dash-dot line with triangles). (a) $\alpha = 0.001$, (b) $\alpha = 0.01$, (c) $\alpha = 0.1$, and (d) $\alpha = 1$.

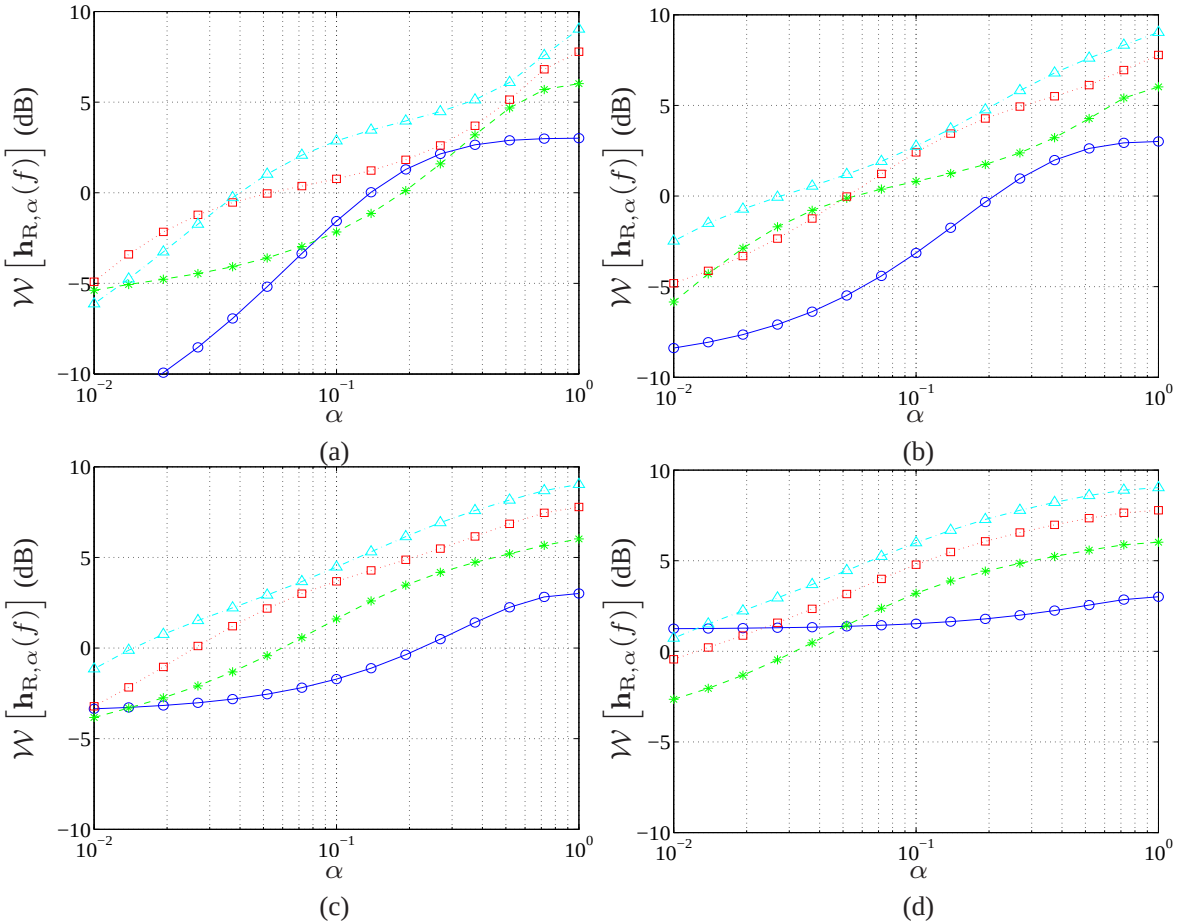


Figure 13: WNG of the robust superdirective beamformer for different numbers of sensors, $M$, and several frequencies: $M = 2$ (solid line with circles), $M = 4$ (dashed line with asterisks), $M = 6$ (dotted line with squares), and $M = 8$ (dash-dot line with triangles). (a) $f = 1$ kHz, (b) $f = 2$ kHz, (c) $f = 4$ kHz, and (d) $f = 8$ kHz.

Figure 14 shows plots of the DF, $\mathcal{D}\left[\mathbf{h}_{\mathrm{R},\alpha}(f)\right]$, as a function of frequency, for different numbers of sensors, $M$, and several values of $\alpha$.

Figure 15 shows plots of the DF, $\mathcal{D}\left[\mathbf{h}_{\mathrm{R},\alpha}(f)\right]$, as a function of $\alpha$, for different numbers of sensors, $M$, and several frequencies.

For given frequency and $\alpha$, as the number of sensors increases, the DF of the robust superdirective beamformer increases.

For given frequency and $M$, as the value of $\alpha$ increases, the WNG of the robust superdirective beamformer increases at the expense of a lower DF.

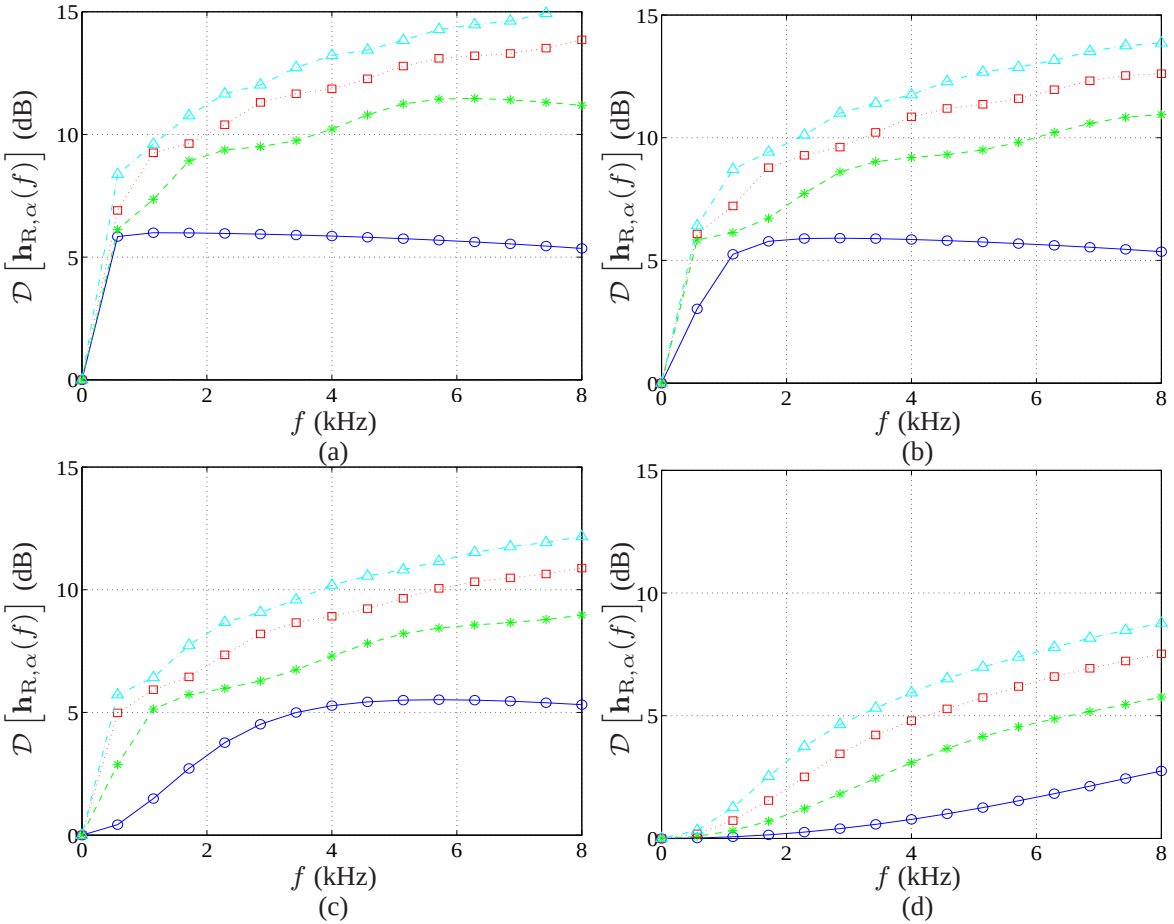


Figure 14: DF of the robust superdirective beamformer for different numbers of sensors, $M$, and several values of $\alpha$: $M = 2$ (solid line with circles), $M = 4$ (dashed line with asterisks), $M = 6$ (dotted line with squares), and $M = 8$ (dash-dot line with triangles). (a) $\alpha = 0.001$, (b) $\alpha = 0.01$, (c) $\alpha = 0.1$, and (d) $\alpha = 1$.

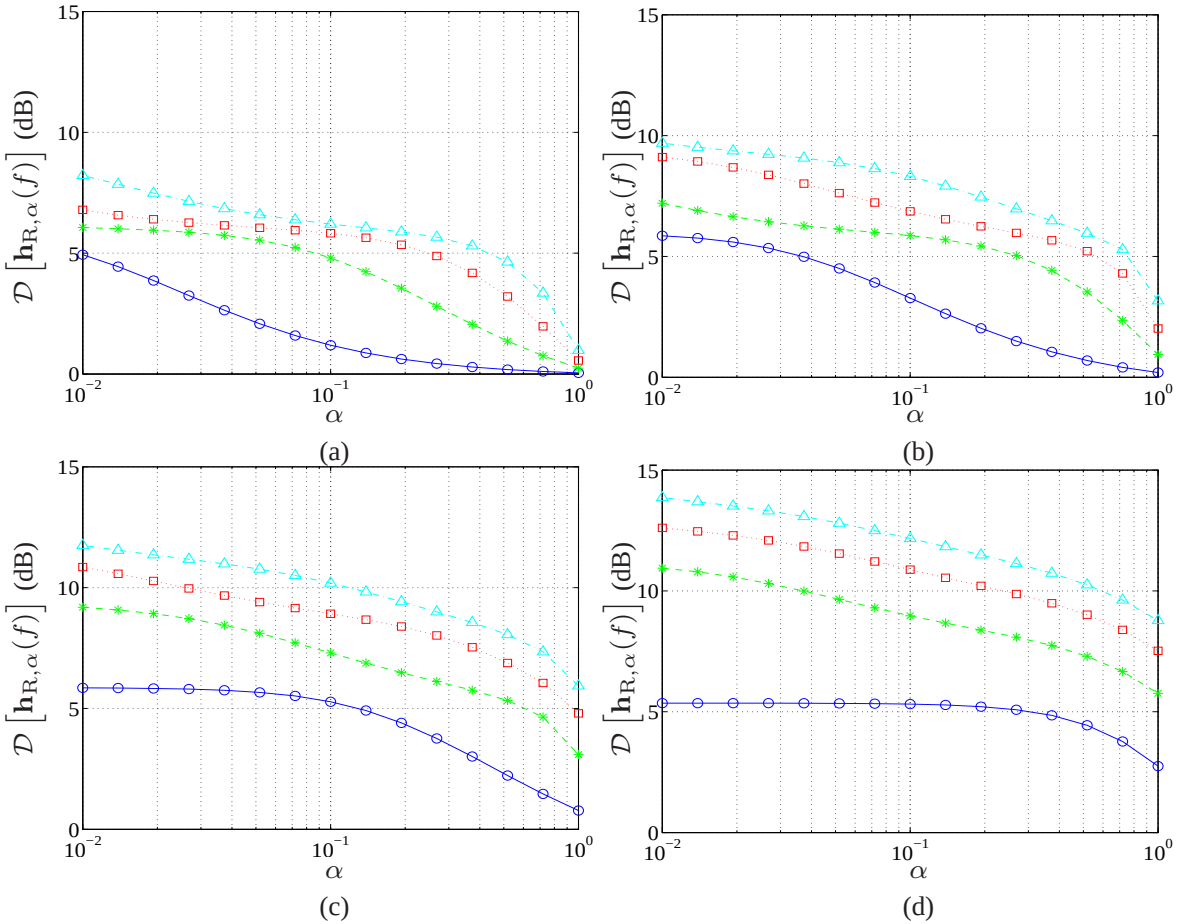


Figure 15: DF of the robust superdirective beamformer for different numbers of sensors, $M$, and several frequencies: $M = 2$ (solid line with circles), $M = 4$ (dashed line with asterisks), $M = 6$ (dotted line with squares), and $M = 8$ (dash-dot line with triangles). (a) $f = 1$ kHz, (b) $f = 2$ kHz, (c) $f = 4$ kHz, and (d) $f = 8$ kHz.

Figures 16–18 show beampatterns, $|\mathcal{B}[\mathbf{h}_{\mathrm{R},\alpha}(f), \cos\theta]|$, for $M = 8$, several values of $\alpha$, and several frequencies.

The main beam is in the direction of the desired signal, i.e., $\theta_{\mathrm{d}} = 0°$.

For a given $\alpha$, as the frequency increases, the width of the main beam decreases.

For a given frequency, as the value of $\alpha$ increases, the width of the main beam increases (lower DF).

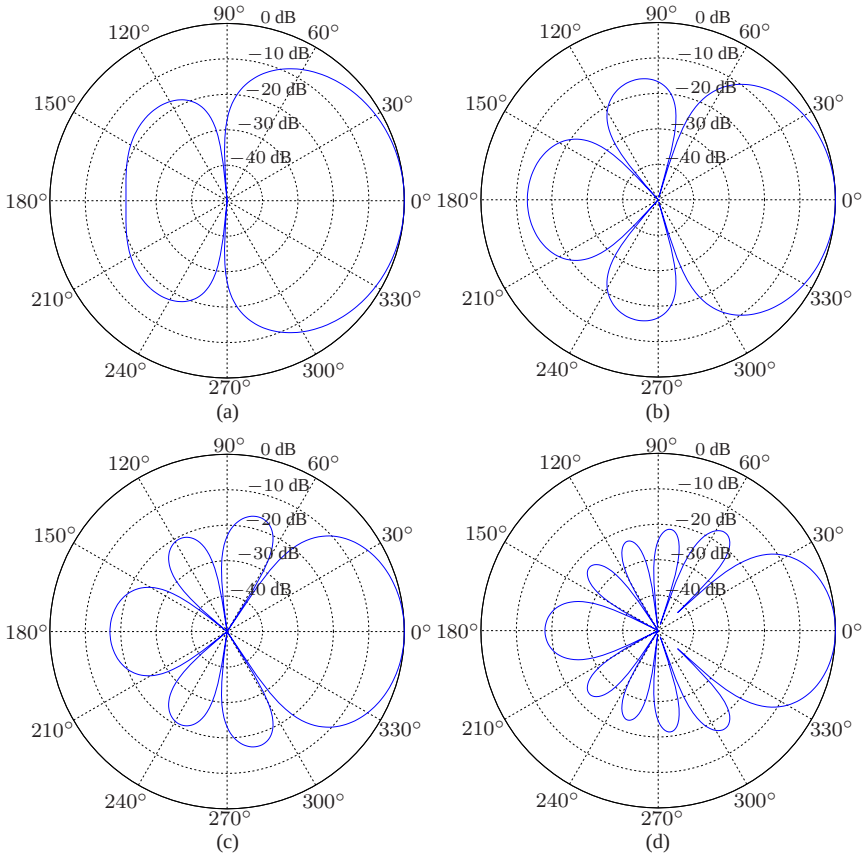


Figure 16: Beampatterns of the robust superdirective beamformer for $\alpha = 0.01$ and several frequencies: (a) $f = 1$ kHz, (b) $f = 2$ kHz, (c) $f = 4$ kHz, and (d) $f = 8$ kHz.

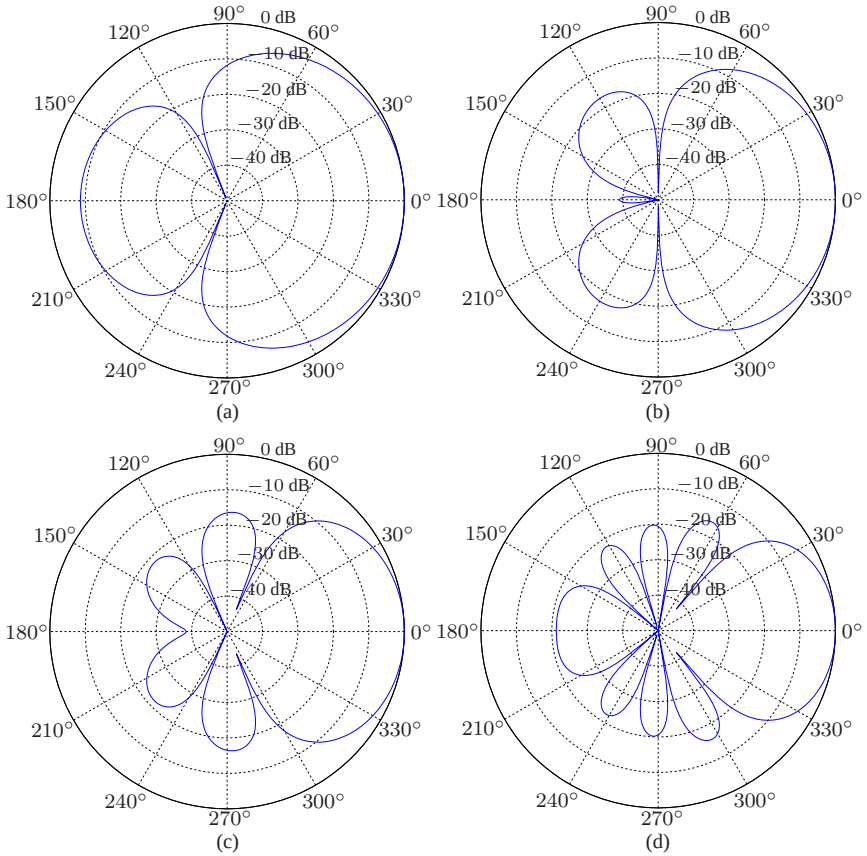


Figure 17: Beampatterns of the robust superdirective beamformer for $\alpha = 0.1$ and several frequencies: (a) $f = 1$ kHz, (b) $f = 2$ kHz, (c) $f = 4$ kHz, and (d) $f = 8$ kHz.

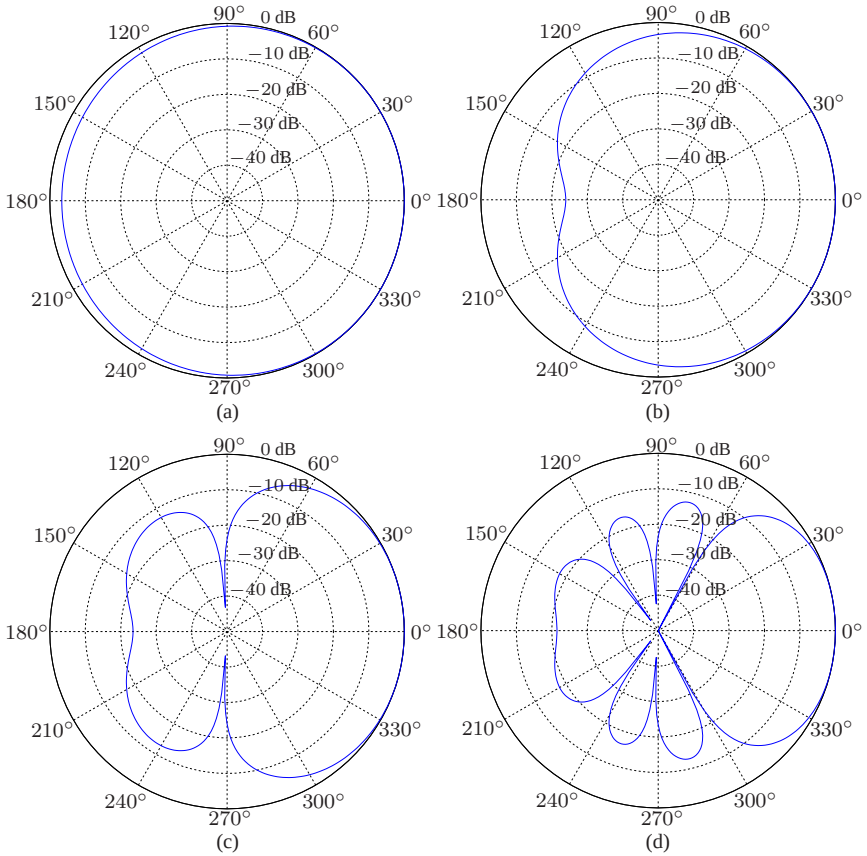


Figure 18: Beampatterns of the robust superdirective beamformer for $\alpha = 1$ and several frequencies: (a) $f = 1$ kHz, (b) $f = 2$ kHz, (c) $f = 4$ kHz, and (d) $f = 8$ kHz.

Let $\mathbf{A}$ and $\mathbf{B}$ two invertible square matrices.

If $\epsilon$ is small compared to $\mathbf{A}$ and $\mathbf{B}$, then [13]

$$(\mathbf{A}+\epsilon\mathbf{B})^{-1} \approx \mathbf{A}^{-1} - \epsilon\mathbf{A}^{-1}\mathbf{B}\mathbf{A}^{-1}. \tag{85}$$

Using the previous approximation in $\mathbf{\Gamma}_{\alpha}(f)$, we get

$$\mathbf{\Gamma}_{\alpha}(f) \approx (1-\alpha)^{-2}\mathbf{\Gamma}_{0,\pi}^{-1}(f)\mathbf{\Gamma}_{\alpha^-}(f)\mathbf{\Gamma}_{0,\pi}^{-1}(f) \tag{86}$$

for $0 \leq \alpha \leq 0.5$, and

$$\mathbf{\Gamma}_{\alpha}(f) \approx -\alpha^{-2}\mathbf{\Gamma}_{\alpha^-}(f) \tag{87}$$

for $0.5 < \alpha \leq 1$, where

$$\mathbf{\Gamma}_{\alpha^-}(f) = [1-\alpha(f)]\,\mathbf{\Gamma}_{0,\pi}(f) - \alpha(f)\mathbf{I}_M. \tag{88}$$

As a result, the robust beamformer becomes

$$\mathbf{h}_{\mathrm{R},\alpha\leq 0.5}(f)=\frac{\mathbf{\Gamma}_{0,\pi}^{-1}(f)\mathbf{\Gamma}_{\alpha-}(f)\mathbf{\Gamma}_{0,\pi}^{-1}(f)\mathbf{d}\left(f,1\right)}{\mathbf{d}^{H}\left(f,1\right)\mathbf{\Gamma}_{0,\pi}^{-1}(f)\mathbf{\Gamma}_{\alpha-}(f)\mathbf{\Gamma}_{0,\pi}^{-1}(f)\mathbf{d}\left(f,1\right)}, \tag{89}$$

$$\mathbf{h}_{\mathrm{R},\alpha>0.5}(f)=\frac{\mathbf{\Gamma}_{\alpha-}(f)\mathbf{d}\left(f,1\right)}{\mathbf{d}^{H}\left(f,1\right)\mathbf{\Gamma}_{\alpha-}(f)\mathbf{d}\left(f,1\right)}. \tag{90}$$

We deduce that the WNG and the DF are, respectively,

$$\mathcal{W}\left[\mathbf{h}_{\mathrm{R},\alpha\leq 0.5}(f)\right]= \frac{\left[\mathbf{d}^{H}\left(f,1\right)\mathbf{\Gamma}_{0,\pi}^{-1}(f)\mathbf{\Gamma}_{\alpha-}(f)\mathbf{\Gamma}_{0,\pi}^{-1}(f)\mathbf{d}\left(f,1\right)\right]^{2}}{\mathbf{d}^{H}\left(f,1\right)\mathbf{\Gamma}_{0,\pi}^{-1}(f)\mathbf{\Gamma}_{\alpha-}(f)\mathbf{\Gamma}_{0,\pi}^{-2}(f)\mathbf{\Gamma}_{\alpha-}(f)\mathbf{\Gamma}_{0,\pi}^{-1}(f)\mathbf{d}\left(f,1\right)}, \tag{91}$$

$$\mathcal{W}\left[\mathbf{h}_{\mathrm{R},\alpha>0.5}(f)\right]=\frac{\left[\mathbf{d}^{H}\left(f,1\right)\mathbf{\Gamma}_{\alpha-}(f)\mathbf{d}\left(f,1\right)\right]^{2}}{\mathbf{d}^{H}\left(f,1\right)\mathbf{\Gamma}_{\alpha-}^{2}(f)\mathbf{d}\left(f,1\right)}, \tag{92}$$

and

$$\mathcal{D}\left[\mathbf{h}_{\mathrm{R},\alpha\leq 0.5}(f)\right] = \frac{\left[\mathbf{d}^H(f,1)\,\mathbf{\Gamma}_{0,\pi}^{-1}(f)\mathbf{\Gamma}_{\alpha-}(f)\mathbf{\Gamma}_{0,\pi}^{-1}(f)\mathbf{d}(f,1)\right]^2}{\mathbf{d}^H(f,1)\,\mathbf{\Gamma}_{0,\pi}^{-1}(f)\mathbf{\Gamma}_{\alpha-}(f)\mathbf{\Gamma}_{0,\pi}^{-1}(f)\mathbf{\Gamma}_{\alpha-}(f)\mathbf{\Gamma}_{0,\pi}^{-1}(f)\mathbf{d}(f,1)}, \tag{93}$$

$$\mathcal{D}\left[\mathbf{h}_{\mathrm{R},\alpha>0.5}(f)\right] = \frac{\left[\mathbf{d}^H(f,1)\,\mathbf{\Gamma}_{\alpha-}(f)\mathbf{d}(f,1)\right]^2}{\mathbf{d}^H(f,1)\,\mathbf{\Gamma}_{\alpha-}(f)\mathbf{\Gamma}_{0,\pi}(f)\mathbf{\Gamma}_{\alpha-}(f)\mathbf{d}(f,1)}. \tag{94}$$

The good thing about this approximation is that for a desired WNG or DF, we can find the corresponding value of $\alpha(f)$.

# Null Steering

In this subsection, we assume that we have $N$ sources, with $N < M$, impinging on the array from the directions $\theta_1 \neq \theta_2 \neq \cdots \neq \theta_N \neq \theta_{\mathrm{d}}$.

These sources are considered as interferences that we would like to completely cancel, i.e., to put nulls in the directions $\theta_n,\ n = 1, 2, \ldots, N$, with a beamformer $\mathbf{h}(f)$, and, meanwhile, recover the desired source coming from the direction $\theta_{\mathrm{d}}$.

Combining all these constraints together, we get the constraint equation:

$$\mathbf{C}^H\left(f, \theta_{\mathrm{d}}, \theta_{1:N}\right)\mathbf{h}(f) = \mathbf{i}_{\mathrm{c}}, \tag{95}$$

where

$$\mathbf{C}\left(f,\theta_{\mathrm{d}},\theta_{1:N}\right)=\left[\begin{array}{cccc}\mathbf{d}\left(f,\theta_{\mathrm{d}}\right) & \mathbf{d}\left(f,\theta_{1}\right) & \cdots & \mathbf{d}\left(f,\theta_{N}\right)\end{array}\right] \tag{96}$$

is the constraint matrix of size $M\times(N+1)$ whose $N+1$ columns are linearly independent and

$$\mathbf{i}_{\mathrm{c}}=\left[\begin{array}{cccc}1 & 0 & \cdots & 0\end{array}\right]^{T} \tag{97}$$

is a vector of length $N+1$.

Depending on what it is desired, we have at least two different approaches to find the optimal filter, which are based on the WNG and the DF as criteria.

The first obvious beamformer is obtained by maximizing the WNG and by taking (95) into account, i.e.,

$$\min_{\mathbf{h}(f)} \mathbf{h}^H(f)\mathbf{h}(f) \quad \text{subject to} \quad \mathbf{C}^H\left(f,\theta_{\mathrm{d}},\theta_{1:N}\right)\mathbf{h}(f)=\mathbf{i}_{\mathrm{c}}. \tag{98}$$

From this criterion, we find the minimum-norm (MN) beamformer:

$$\mathbf{h}_{\mathrm{MN}}\left(f,\cos\theta_{\mathrm{d}}\right)=\mathbf{C}\left(f,\theta_{\mathrm{d}},\theta_{1:N}\right)\left[\mathbf{C}^H\left(f,\theta_{\mathrm{d}},\theta_{1:N}\right)\mathbf{C}\left(f,\theta_{\mathrm{d}},\theta_{1:N}\right)\right]^{-1}\mathbf{i}_{\mathrm{c}}, \tag{99}$$

which is also the minimum-norm solution of (95).

Clearly, we always have

$$\mathcal{W}\left[\mathbf{h}_{\mathrm{MN}}\left(f,\cos\theta_{\mathrm{d}}\right)\right]\leq\mathcal{W}\left[\mathbf{h}_{\mathrm{DS}}\left(f,\cos\theta_{\mathrm{d}}\right)\right]. \tag{100}$$

The other beamformer is obtained by maximizing the DF and by taking (95) into account, i.e.,

$$\min_{\mathbf{h}(f)} \mathbf{h}^H(f)\mathbf{\Gamma}_{0,\pi}(f)\mathbf{h}(f) \quad \text{subject to} \quad \mathbf{C}^H\left(f,\theta_{\mathrm{d}},\theta_{1:N}\right)\mathbf{h}(f)=\mathbf{i}_{\mathrm{c}}. \tag{101}$$

We easily find the null-steering (NS) beamformer:

$$\mathbf{h}_{\mathrm{NS}}\left(f,\cos\theta_{\mathrm{d}}\right)=\mathbf{\Gamma}_{0,\pi}^{-1}(f)\mathbf{C}\left(f,\theta_{\mathrm{d}},\theta_{1:N}\right)\times \left[\mathbf{C}^H\left(f,\theta_{\mathrm{d}},\theta_{1:N}\right)\mathbf{\Gamma}_{0,\pi}^{-1}(f)\mathbf{C}\left(f,\theta_{\mathrm{d}},\theta_{1:N}\right)\right]^{-1}\mathbf{i}_{\mathrm{c}}. \tag{102}$$

Obviously, we always have

$$\mathcal{D}\left[\mathbf{h}_{\mathrm{NS}}\left(f,\cos\theta_{\mathrm{d}}\right)\right]\leq\mathcal{D}\left[\mathbf{h}_{\mathrm{mDF}}\left(f,\cos\theta_{\mathrm{d}}\right)\right]. \tag{103}$$

A straightforward way to compromise between the WNG and the DF with the null-steering approach is the following beamformer:

$$\mathbf{h}_{\alpha}\left(f,\cos\theta_{\mathrm{d}}\right)=\boldsymbol{\Gamma}_{\alpha}^{-1}(f)\mathbf{C}\left(f,\theta_{\mathrm{d}},\theta_{1:N}\right)\times \left[\mathbf{C}^{H}\left(f,\theta_{\mathrm{d}},\theta_{1:N}\right)\boldsymbol{\Gamma}_{\alpha}^{-1}(f)\mathbf{C}\left(f,\theta_{\mathrm{d}},\theta_{1:N}\right)\right]^{-1}\mathbf{i}_{\mathrm{c}}, \quad (104)$$

where $\boldsymbol{\Gamma}_{\alpha}(f)$ is defined in (77).

We observe that $\mathbf{h}_{0}\left(f,\cos\theta_{\mathrm{d}}\right)=\mathbf{h}_{\mathrm{NS}}\left(f,\cos\theta_{\mathrm{d}}\right)$ and $\mathbf{h}_{1}\left(f,\cos\theta_{\mathrm{d}}\right)=\mathbf{h}_{\mathrm{MN}}\left(f,\cos\theta_{\mathrm{d}}\right)$.

# Example 4

Returning to Example 1, we now employ the MN/NS beamformer, $\mathbf{h}_\alpha\left(f, \cos\theta_\mathrm{d}\right)$, given in (104).

To demonstrate the performance of the MN/NS beamformer, we choose $\theta_\mathrm{d} = 0°$, $\theta_1 = 45°$, $\theta_2 = 90°$, and $\delta = 1$ cm.

Figure 19 shows plots of the WNG, $\mathcal{W}\left[\mathbf{h}_\alpha\left(f, \cos\theta_\mathrm{d}\right)\right]$, as a function of frequency, for different numbers of sensors, $M$, and several values of $\alpha$.

As a reference, the WNG of the DS beamformer, $\mathcal{W}\left[\mathbf{h}_\mathrm{DS}\left(f, \cos\theta_\mathrm{d}\right)\right]$, is also plotted.

For given frequency and $M$, as the value of $\alpha$ increases, the WNG of the MN/NS beamformer increases, and is upper bounded by the WNG of the DS beamformer.

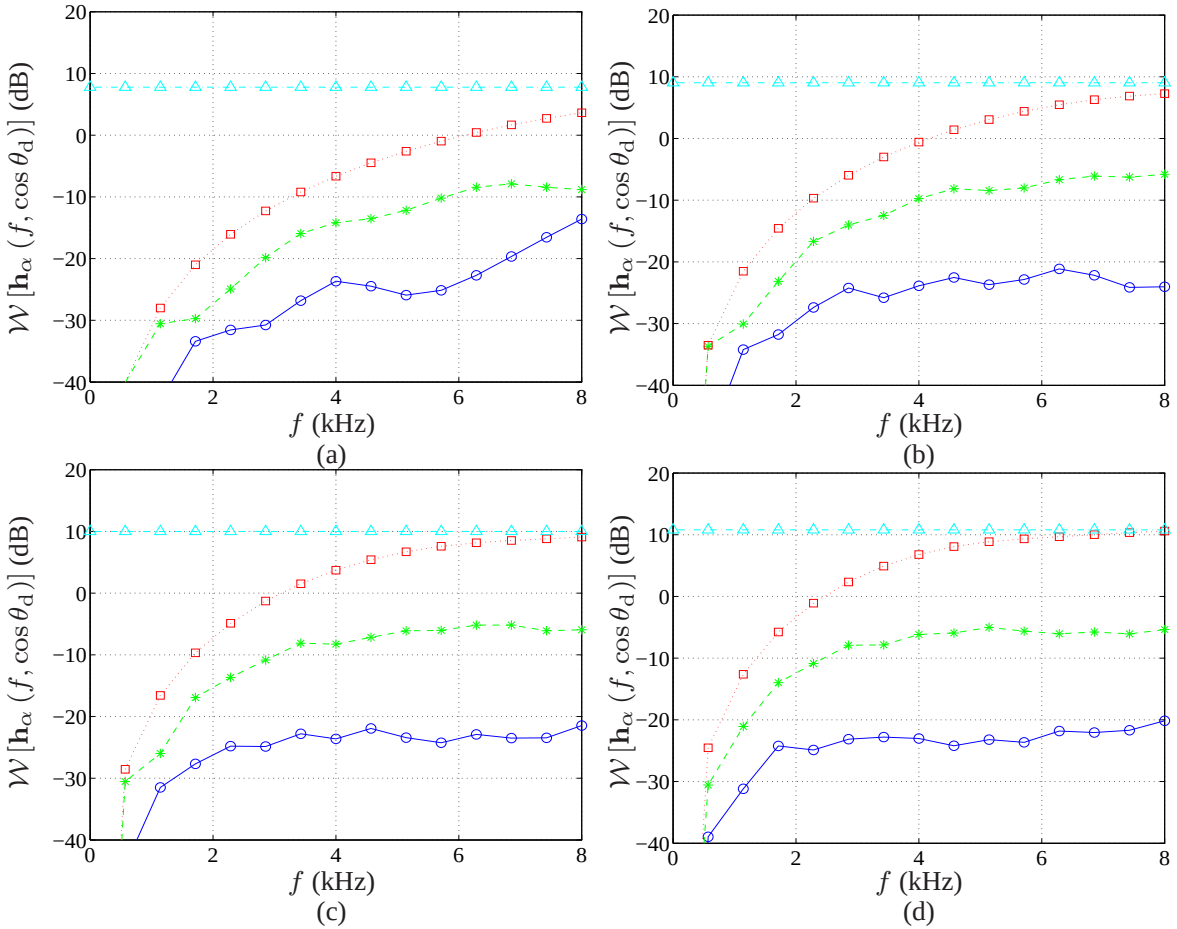


Figure 19: WNG of the MN/NS beamformer for different $M$ and $\alpha$ values: $\alpha = 1e-5$ (solid line with circles), $\alpha = 1e-3$ (dashed line with asterisks), and $\alpha = 1$ (dotted line with squares). (a) $M = 6$, (b) $M = 8$, (c) $M = 10$, and (d) $M = 12$. As a reference, $\mathcal{W}[\mathbf{h}_{\mathrm{DS}}(f,\cos\theta_d)]$ is also plotted in the figures (dash-dot line with triangles).

Figure 20 shows plots of the DF, $\mathcal{D}\left[\mathbf{h}_{\alpha}\left(f,\cos\theta_{\mathrm{d}}\right)\right]$, as a function of frequency, for different numbers of sensors, $M$, and several values of $\alpha$.

As a reference, the DF of the maximum DF beamformer, $\mathcal{D}\left[\mathbf{h}_{\mathrm{mDF}}\left(f,\cos\theta_{\mathrm{d}}\right)\right]$, is also plotted.

For given frequency and $M$, as the value of $\alpha$ increases, the DF of the MN/NS beamformer decreases, and is upper bounded by the WNG of the maximum DF beamformer.

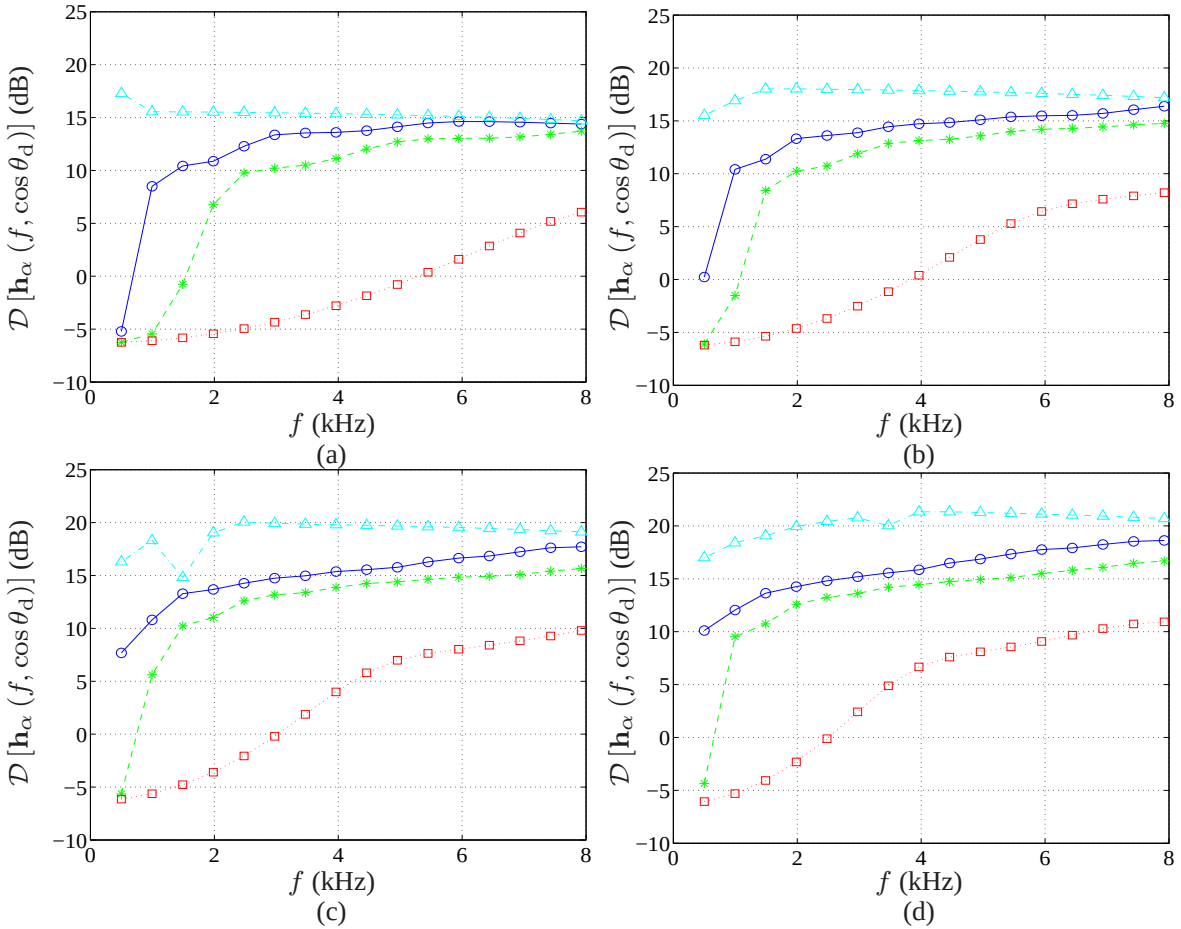


Figure 20: DF of the MN/NS beamformer for different $M$ and $\alpha$ values: $\alpha = 1e-5$ (solid line with circles), $\alpha = 1e-3$ (dashed line with asterisks), and $\alpha = 1$ (dotted line with squares). (a) $M = 6$, (b) $M = 8$, (c) $M = 10$, and (d) $M = 12$. As a reference, $\mathcal{D}[\mathbf{h}_{\mathrm{mDF}}(f,\cos\theta_d)]$ is also plotted in the figures (dash-dot line with triangles).

Figures 21–23 show beampatterns, $|\mathcal{B}\left[\mathbf{h}_\alpha\left(f, \cos\theta_\mathrm{d}\right), \cos\theta\right]|$, for $M = 8$, several values of $\alpha$, and several frequencies.

The main beam is in the direction of the desired signal, i.e., $\theta_\mathrm{d}$.

Compared to the previous beamformers, here the width of the main beam is less sensitive to frequency.

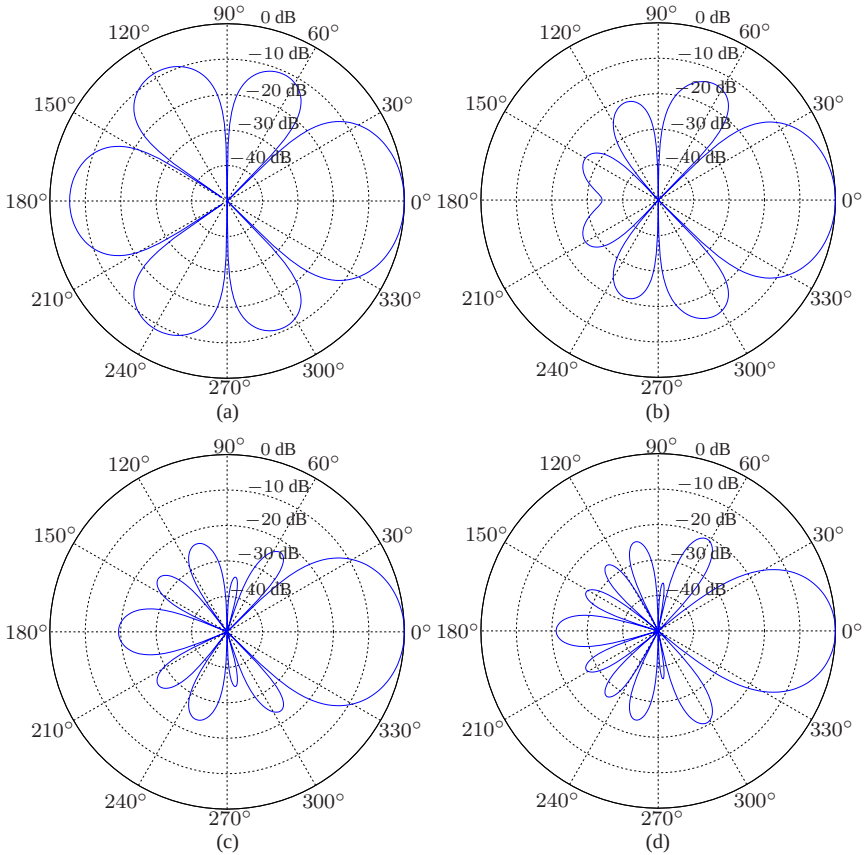


Figure 21: Beampatterns of the MN/NS beamformer for several frequencies with $M = 8$ and $\alpha = 1e - 5$: (a) $f = 1$ kHz, (b) $f = 2$ kHz, (c) $f = 4$ kHz, and (d) $f = 8$ kHz.

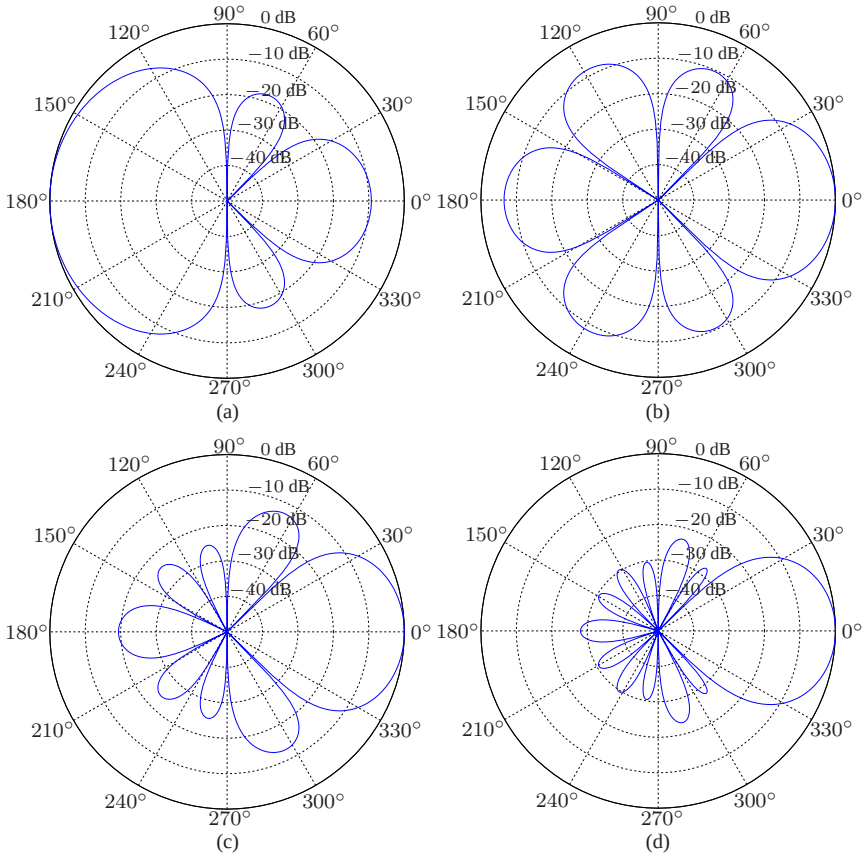


Figure 22: Beampatterns of the MN/NS beamformer for several frequencies with $M = 8$ and $\alpha = 1e - 3$: (a) $f = 1$ kHz, (b) $f = 2$ kHz, (c) $f = 4$ kHz, and (d) $f = 8$ kHz.

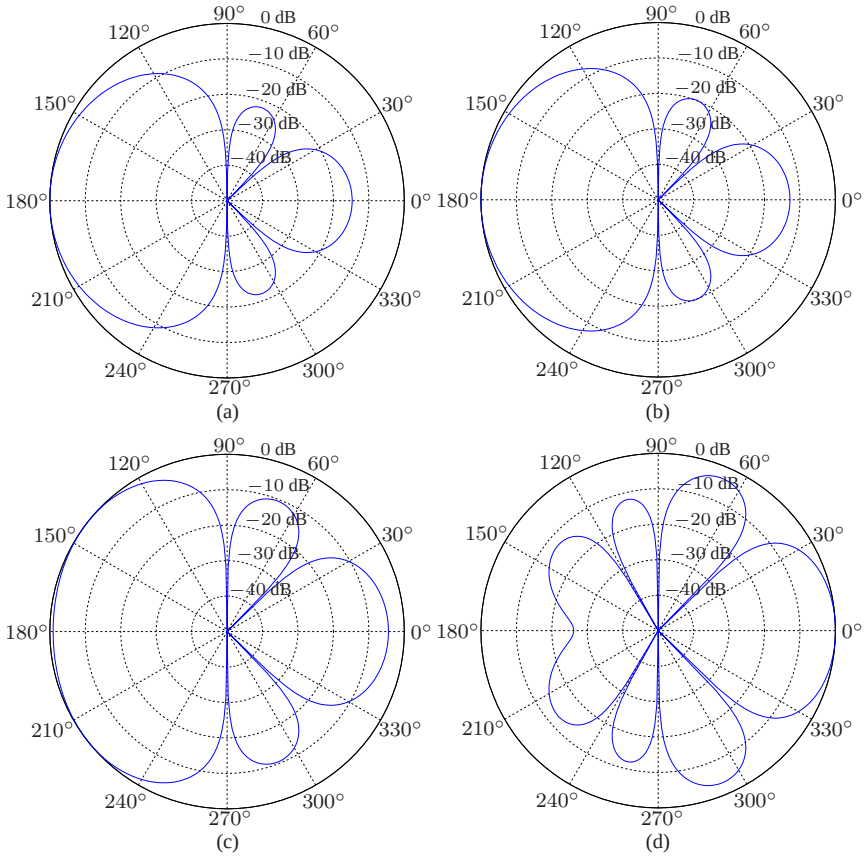


Figure 23: Beampatterns of the MN/NS beamformer for several frequencies with $M = 8$ and $\alpha = 1$: (a) $f = 1$ kHz, (b) $f = 2$ kHz, (c) $f = 4$ kHz, and (d) $f = 8$ kHz.

In the table below we summarize all the fixed beamformers studied in this section:

| | |
|---|---|
| DS: | $\mathbf{h}_{\mathrm{DS}}\left(f,\cos\theta_{\mathrm{d}}\right)=\dfrac{\mathbf{d}\left(f,\cos\theta_{\mathrm{d}}\right)}{M}$ |
| Maximum DF: | $\mathbf{h}_{\mathrm{mDF}}\left(f,\cos\theta_{\mathrm{d}}\right)=\dfrac{\boldsymbol{\Gamma}_{0,\pi}^{-1}(f)\mathbf{d}\left(f,\cos\theta_{\mathrm{d}}\right)}{\mathbf{d}^{H}\left(f,\cos\theta_{\mathrm{d}}\right)\boldsymbol{\Gamma}_{0,\pi}^{-1}(f)\mathbf{d}\left(f,\cos\theta_{\mathrm{d}}\right)}$ |
| Superdirective: | $\mathbf{h}_{\mathrm{SD}}(f)=\dfrac{\boldsymbol{\Gamma}_{0,\pi}^{-1}(f)\mathbf{d}\left(f,1\right)}{\mathbf{d}^{H}\left(f,1\right)\boldsymbol{\Gamma}_{0,\pi}^{-1}(f)\mathbf{d}\left(f,1\right)}$ |
| Robust SD: | $\mathbf{h}_{\mathrm{R},\alpha}(f)=\dfrac{\boldsymbol{\Gamma}_{\alpha}^{-1}(f)\mathbf{d}\left(f,1\right)}{\mathbf{d}^{H}\left(f,1\right)\boldsymbol{\Gamma}_{\alpha}^{-1}(f)\mathbf{d}\left(f,1\right)}$ |
| Minimum Norm: | $\mathbf{h}_{\mathrm{MN}}\left(f,\cos\theta_{\mathrm{d}}\right)=\mathbf{C}\left(f,\theta_{\mathrm{d}},\theta_{1:N}\right)\left[\mathbf{C}^{H}\left(f,\theta_{\mathrm{d}},\theta_{1:N}\right)\mathbf{C}\left(f,\theta_{\mathrm{d}},\theta_{1:N}\right)\right]^{-1}\mathbf{i}_{\mathrm{c}}$ |
| Null Steering: | $\mathbf{h}_{\mathrm{NS}}\left(f,\cos\theta_{\mathrm{d}}\right)=\boldsymbol{\Gamma}_{0,\pi}^{-1}(f)\mathbf{C}\left(f,\theta_{\mathrm{d}},\theta_{1:N}\right)\times\left[\mathbf{C}^{H}\left(f,\theta_{\mathrm{d}},\theta_{1:N}\right)\boldsymbol{\Gamma}_{0,\pi}^{-1}(f)\mathbf{C}\left(f,\theta_{\mathrm{d}},\theta_{1:N}\right)\right]^{-1}\mathbf{i}_{\mathrm{c}}$ |
| MN/NS: | $\mathbf{h}_{\alpha}\left(f,\cos\theta_{\mathrm{d}}\right)=\boldsymbol{\Gamma}_{\alpha}^{-1}(f)\mathbf{C}\left(f,\theta_{\mathrm{d}},\theta_{1:N}\right)\times\left[\mathbf{C}^{H}\left(f,\theta_{\mathrm{d}},\theta_{1:N}\right)\boldsymbol{\Gamma}_{\alpha}^{-1}(f)\mathbf{C}\left(f,\theta_{\mathrm{d}},\theta_{1:N}\right)\right]^{-1}\mathbf{i}_{\mathrm{c}}$ |

[1] B. D. Van Veen and K. M. Buckley, “Beamforming: a versatile approach to spatial filtering,” *IEEE Acoust., Speech, Signal Process. Mag.*, vol. 5, pp. 4–24, Apr. 1988.

[2] D. H. Johnson and D. E. Dudgeon, *Array Signal Processing: Concepts and Techniques*. Signal Processing Series. Englewood Cliffs, NJ: Prentice-Hall, 1993.

[3] R. A. Monzingo and T. W. Miller, *Introduction to Adaptive Arrays*. Raleigh, NC: SciTech, 2004.

[4] J. P. Dmochowski and J. Benesty, “Microphone arrays: fundamental concepts,” in *Speech Processing in Modern Communication–Challenges and Perspectives*, I. Cohen, J. Benesty, and S. Gannot, Eds., Berlin, Germany: Springer-Verlag, 2008, Chapter 8, pp. 199–223, 2010.

[5] H. L. Van Trees, *Optimum Array Processing: Part IV of Detection, Estimation, and Modulation Theory*. New York, NY: John Wiley & Sons, Inc., 2002.

[6] R. Berkun, I. Cohen, and J. Benesty, “Combined beamformers for robust broadband regularized superdirective beamforming,” *IEEE/ACM Trans. Audio, Speech, Language Process.*, vol. 23, pp. 877–886, May 2015.

[7] G. A. F. Seber, *A Matrix Handbook for Statisticians*. Hoboken, NJ: John Wiley & Sons, Inc., 2008.

[8] C. Pan, J. Chen, and J. Benesty, "Performance study of the MVDR beamformer as a function of the source incidence angle," *IEEE/ACM Trans. Audio, Speech, Language Process.*, vol. 22, pp. 67–79, Jan. 2014.

[9] J. M. Kates and M. R. Weiss, "A comparison of hearing-aid array-processing techniques," *J. Acoust. Soc. Am.*, vol. 99, pp. 3138–3148, May 1996.

[10] A. I. Uzkov, "An approach to the problem of optimum directive antenna design," *Comptes Rendus (Doklady) de l'Academie des Sciences de l'URSS*, vol. LIII, no. 1, pp. 35–38, 1946.

[11] H. Cox, R. M. Zeskind, and T. Kooij, "Practical supergain," *IEEE Trans. Acoust., Speech, Signal Process.*, vol. ASSP-34, pp. 393–398, June 1986.

[12] H. Cox, R. M. Zeskind, and M. M. Owen, "Robust adaptive beamforming," *IEEE Trans. Acoust., Speech, Signal Process.*, vol. ASSP-35, pp. 1365–1376, Oct. 1987.

[13] K. B. Petersen and M. S. Pedersen, *The Matrix Cookbook*. http://matrixcookbook.com, 2012.

[14] J. N. Franklin, *Matrix Theory*. Englewood Cliffs, NJ: Prentice-Hall, 1968.